UPPSALA
UNIVERSITET

Digital Comprehensive Summaries of Uppsala Dissertations from the Faculty of Science and Technology 1119

Structure and Electronic Properties of Phthalocyanine Films on Metal and Semiconductor Substrates

IEVA BIDERMANE

ACTA
UNIVERSITATIS
UPSALIENSIS
UPPSALA
2014

ISSN 1651-6214
ISBN 978-91-554-8867-3
urn:nbn:se:uu:diva-217086

Dissertation presented at Uppsala University to be publicly examined in Häggsalen, Ångström Laboratory, Lägerhyddsvägen 1, Uppsala, Friday, 14 March 2014 at 10:15 for the degree of Doctor of Philosophy. The examination will be conducted in English. Faculty examiner: Luca Giovanelli (Aix-Marseille Universite).

Abstract

Bidermane, I. 2014. Structure and Electronic Properties of Phthalocyanine Films on Metal and Semiconductor Substrates. *Digital Comprehensive Summaries of Uppsala Dissertations from the Faculty of Science and Technology* 1119. 51 pp. Uppsala: Acta Universitatis Upsaliensis. ISBN 978-91-554-8867-3.

The current thesis presents fundamental studies of phthalocyanines (Pcs), a group of organic macro-cycle molecules. The use of phthalocyanine molecular films in devices with a variety of possible technological applications has been the reason of the many studies dedicated to such molecules during the last decades.

Core and valence photoelectron spectroscopies (PES), X-ray absorption spectroscopy (XAS) and scanning tunneling microscopy (STM) techniques are used to study phthalocyanine molecules in gas phase and adsorbed on gold (111) and silicon Si(100)-2x1 substrates. Density functional theory (DFT) is used to obtain further insights in the electronic structure of the phthalocyanines.

The aim of our studies is to get a deeper understanding into the molecule-molecule and molecule-substrate interactions, a fundamental requirement for improving the devices based on such molecular materials.

Gas phase PES and XAS studies and single molecule DFT calculations are performed on the valence band (VB) of iron phthalocyanine (FePc), manganese phthalocyanine (MnPc) and metal-free phthalocyanine (H_2Pc). The VB simulations have shown how the metal atom of the Pc influences the inner valence states of the molecules. The HOMO of the H_2Pc and FePc is formed by mostly C2p states, whereas the HOMO of MnPc has mainly Mn3d character.

PES studies of H_2Pc on Au(111) have revealed the influence of the surface on the adsorption of the monolayer. XAS studies indicate formation of ordered monolayer with the Pc ligands parallel to the surface and the change of the molecular tilt angle with increasing thicknesses. For $LuPc_2$ adsorbed on Au(111), STM study demonstrates a formation of bilayer instead of a monolayer.

A comparison between the results of $LuPc_2$ adsorbed on pristine or passivated Si(100)-2x1 confirmes the different reactivities of these surfaces: $LuPc_2$ retains many molecular-like characters, when adsorbed on the innert passivated Si. Instead, on the more reactive pristine Si surface, the spectroscopic results have indicated a more significant interaction, possible hybridization and charge redistribution between the molecules and the surface. Moreover, STM images show a modification of the geometrical shape of the molecules, which are proposed to adsorb in two different geometries on the pristine Si surface.

Keywords: Phthalocyanines, silicon(100), Au(111), photoelectron spectroscopy, scanning tunneling microscopy, surface science, organic molecules on surface

Ieva Bidermane, Department of Physics and Astronomy, Molecular and condensed matter physics, Box 516, Uppsala University, SE-751 20 Uppsala, Sweden.

ISSN 1651-6214
ISBN 978-91-554-8867-3
urn:nbn:se:uu:diva-217086 (http://urn.kb.se/resolve?urn=urn:nbn:se:uu:diva-217086)

Opponent: Dr. Luca Giovanelli
Aix-Marseille Université, France

Committee: Prof. Abhay Shukla
Université de Pierre et Marie Curie, France

Prof Anne Borg
Norges Teknisk-Naturvitenskapelige Universitet, Norway

Prof. Mats Fahlman
Linköping University, Sweden

Dr. Barbara Ressel
University of Nova Gorica, Slovenia

Prof. Jan-Erik Rubensson
Uppsala Univeristy, Sweden

List of papers

This thesis is based on the following papers, which are referred to in the text by their Roman numerals.

I **Experimental and Theoretical Study of Electronic Structure of Lutetium bi-Pthalocyanine**
I. Bidermane, J. Lüder, S. Boudet, T. Zhang, S. Ahmadi, C. Grazioli, M. Bouvet, J. Rusz, B. Sanyal, O. Eriksson, B. Brena, C. Puglia, and N. Witkowski. J. Chem. Phys. **138**, 234701 (2013)

II **Adsorption and Molecular Orientation of Lutetium bi-Phthalocyanine Adlayers on Pristine Si(100)-2x1 Surface**
I. Bidermane, S. Ahmadi, C. Grazioli, M. Bouvet, N. Mårtensson, C. Puglia, N. Witkowski, *In manuscript*

III **Photoelectron and Absorption Spectroscopy Studies of Metal-Free Phthalocyanine on Au(111): Experiment and Theory**
M.-N. Shariati, J. Lüder, I. Bidermane, S. Ahmadi, E. Göthelid, P. Palmgren, B. Sanyal, O. Eriksson, M. N. Piancastelli, B. Brena, and C. Puglia. J. Phys. Chem. C, **117**, 7018-7025 (2013)

IV **Formation of Self-organized bi-Layer of Lutetium bi-Phthalocyanine Molecules on Gold (111)**
I. Bidermane, T. Zhang, J. Latvels, K. Pudzs, M. Bouvet, C. Puglia, N. Witkowski, *In manuscript*

V **Characterization of Gas Phase of Iron Phthalocyanine with X-ray Photoelectron and Absorption Spectroscopies**
I. Bidermane, R. Totani, C. Grazioli, M. de Simone, M. Coreno, A. Kivimäki, J. Åhlund, L. Lozzi, C. Puglia, *In manuscript*

VI **Atomic Contributions to the Valence Band Photoelectron Spectra of Metal-free, Iron and Manganese Phthalocyanines**
I. Bidermane, R. Totani, M. N. Shariati, I. Brumboiu, B. Brena, H. C. Herper, O. Eriksson, B. Sanyal, M. de Simone, Antti Kivimaki, C. Grazioli, L. Lozzi, C. Puglia, *In manuscript*

List of papers not included in the thesis

1. **Growth Mode and Self-organization of $LuPc_2$ on Si(001)-2x1 Vicinal Surfaces: An Optical investigation**. S. Boudet, I. Bidermane, E. Lacaze, B. Gallas, M. Bouvet, J. Brunet, A. Pauly, Y. Borensztein, N. Witkowski. Phys. Rev. B, **86**, 115413 (2012)

2. **Aggregation of biphthalocyanines on passivated surfaces : from individual molecules to thick films.** S. Boudet, I. Bidermane, K. Norin, E. Lacaze, M. Bouvet, Y. Borenstein, N. Witkowski, *In Manuscript.*

3. **Effect of the iodine on the self-dependent charge transfer at the Pt(111)-ZnPc interface.** S. Ahmadi, B. Agnarsson, I. Bidermane, Bastian M. Wojek, Quesntin Noel, Mats Göthelid. *Submitted to J. Chem. Phys.*

4. **Dissociative bonding of 4-tert-butyl pyridine on Pt(111) and surface passivation by iodine.** S. Ahmadi, I. Bidermane, Quentin Noel, C. Sun, M. Ghöthelid. *In Manuscript.*

Comments on my own participation

The studies presented in this thesis are a result of teamwork and would be substantially more difficult to accomplish on my own. In Paper I and Paper II, I have been the main responsible for performing the experiments, analyzing the data and writing the manuscript. For remaining papers, I have been mostly involved by participating in the experiments and in data analysis and discussions, as well as partly involved in writing the manuscripts. The theoretical calculations presented here are performed by our collaborators - Johann Lüder, Iulia Brumboiu and Barbara Brena from Materials Theory group at Uppsala University.

Contents

1 Introduction 9

2 Techniques 12
2.1 Photoelectron Spectroscopy 12
2.1.1 Theoretical description of PES 12
2.1.2 Core Levels vs Valence Band 14
2.1.3 Analysis of PES 15
2.2 X-ray Absorption Spectroscopy 15
2.2.1 Principle 16
2.2.2 Acquisition of XAS 17
2.2.3 Molecular orientation 17
2.3 Synchrotron based PE studies 18
2.4 Scanning Tunneling Microscopy 19
2.4.1 Quantum tunneling 19
2.4.2 Operating principle and imaging modes 20

3 Density Functional Theory 22

4 Experimental 23
4.1 From 'real world' to model-system and back 23
4.2 The 'Ultra-High-Vacuum' world 23
4.3 Samples 24
4.3.1 Substrates 24
4.3.2 Phthalocyanines 26
4.4 Experiments at synchrotron facilities 28
4.5 Energy calibration of XPS and XAS spectra 28
4.6 Thickness estimations 29
4.7 Scanning tunneling microscopy 30

5 Summary of Papers 31
5.1 Adlayers of phthalocyanines on surfaces 31
5.1.1 $LuPc_2$ on Si(100)-2×1 surface 31
5.1.2 $LuPc_2$ on Au(111) surface 34
5.1.3 H_2Pc on Au(111) surface 35
5.2 Gas phase experiments 38
5.3 Valence band and the influence of the central metal atom in phthalocyanines. 38
5.4 Conclusions 40

6 Summary in Swedish 42
7 Abstract in French 45
8 Acknowledgments 46
References 48

1. Introduction

For a long time people have turned to nature and tried to understand how she does the things in a such effective and amazing way. People have also realized that even though the nature can do all those things with ease, it is considerably harder when one tries to mimic them and attempt to use the same mechanisms and methods in a man-made device. For the last decades, scientists have been working on creating nano-size devices where a few or even a single molecule device could perform a task now carried out by macroscopic devices. However, in going down to nano-size devices one arrives in a world, where slightly different rules apply and we have to 'learn and understand' these new rules in order to profit from the advantages that this 'new world' can give us. Scientists quickly realized that one could not use the same measurement tools that were used for macrosize science, hence new techniques have been invented that are able to characterize these new systems (microscopy with atomic resolution, femtosecond lasers to be able to follow ultra-fast processes and many others). In general one can distinguish different approaches or ways of contributing to the advancement of these devices.

In order to succeed in making such gadgets we need people advancing in different steps of developement - we need people making the machines and techniques that would allow us to look closer, deeper, faster and we need to understand how to use those techniques characterizing our systems. We need people working on constructing practical devices as well as people that work on characterizing those devices. These are few of the possibly needed steps which are crucial to obtain a final nano-size device that would be competitive in the current market.

Why Phthalocyanines?

Phthalocyanines have attracted attention since their accidental discovery more than a century ago [1] and had directly found use in industrial applications as colorants and dyes. For the last few decades these organic macrocycle molecules have found other potential applications [2] as promising materials in numerous fields such as alternative energy (solar cells [3], enviromental physics (gas sensors [4, 5, 6, 7], organic light emitting diodes [8]) and medicine [9] to name a few. The reason why they are so widely studied is in their similarities to systems one can find in nature, porphyrins, that form the basis of many biologically important systems e.g. hemoglobin, chlorophyll, which again are systems that researchers try to emulate for man-made devices. If one tracks the publications concerning phthalocyanines in the past century, a trend of doubling the number of publications with every decade is

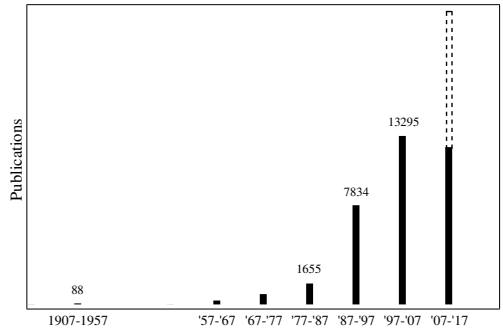

Figure 1.1. Number of publications on Phthalocyanines in the past century [10].

seen (see Fig. 1.1). The additional increase in the number of publications in the last 30 years can be attributed to the advances made in the development of new instrumentation, such as synchrotron facilities and experimental methods like different scanning probe techniques in spectroscopy.

The core interest that led me to phthalocyanine research was the possibility to incorporate of these macro molecules in gas sensors based on the organic field effect transistor model, using phthalocyanines as active sensing layers. There has been considerable research done on the subject [11, 12, 13, 14, 15, 16, 17], however the efficiency (and together with that the competitiveness) are still far behind the conventional devices. The main idea was that understanding the underlying processes at the fundamental level could give additional information on how to improve the efficiency of the sensor. However, studying real systems is a very challenging and sometimes nearly impossible task. This forces scientists to come up with model systems, which are simplified systems that allow better control and separation of the different parameters in order to pinpoint the desired characteristics under study. This is exactly what I did in my thesis: we made a study of model systems, where different types of Pcs were studied under a controlled enviroment.

Studies were performed on two metal phthalocyanines (MPcs) - iron phthalocyanine (FePc) and lutetium biphthalocyanine ($LuPc_2$). Lutetium biphthalocyanine is considered to be one of the promising materials in gas sensor applications [6, 18, 19, 20] because of its redox characteristics, whereas FePc is considered a good catalyst in oxygen reduction reactions [21, 22, 23, 24]). It is still unclear what characteristics govern these processes, however the research presented in this thesis is a crucial step in the direction of being able to answer these questions.

The thesis is made out of five main chapters. Chapter 2 is dedicated to the theoretical background of techniques used in this thesis. Chapter 3 provides a short description of the theoretical calculations that have been used to provide additional information to the experimental results presented here. In Chapter 4 the description of the studied systems - substrates and adsorbates is presented

together with discussions about some practical experimental data analysis related issues. Finally Chapter 5 presents the summary of the papers included in this thesis and final conclusions.

2. Techniques

In this thesis several soft X-ray spectroscopy techniques have been used to characterize the electronic structure and geometry of the materials. In the following sections their principles will be presented.

2.1 Photoelectron Spectroscopy

In photoelectron spectroscopy (PES) the sample is irradated with photons having a well-defined energy $h\nu$. In a photon absorption process the energy can be transferred to an electron, which can gain sufficient energy to be either excited to a higher energy bound state, or to leave the sample. By measuring the kinetic energy E_k of the photoelectron ejected from the sample, it is possible to determine the binding energy of the electronic level:

$$E_B = h\nu - E_k - \phi \tag{2.1}$$

where ϕ is the work function of the material under study (representing the energy difference between the Fermi level and vacuum level), E_B is the binding energy measured from the Fermi edge and E_k is the kinetic energy relative to the vacuum level. PES is an element specific technique since each element has a unique pattern of core levels, each having distinct binding energies, allowing one to obtain the information about the chemical composition of the studied systems. PES is also a surface sensitive technique due to the small escape depth of the photoexcited electrons. Inelastic mean free path (IMFP)[1] distances for kinetic energies ranging from 1-1000 eV[25] are roughly in the nanometer scale or less, as PES provides information mainly about the outermost surface layers.

2.1.1 Theoretical description of PES

2.1.1.1 Fermi's Golden Rule

PES experiments provide information about the difference between the inital and the final states of a system. The transition probability w_{if} for an electron

[1] Escape depth d is related to IMFP as $d = \Delta cos\theta$, where Δ is IMFP and θ is the angle between the detection angle of the emitted electrons and surface normal.

coming from initial state $|i>$ to a final state $|f>$ can be expressed using Fermi's 'Golden Rule':

$$w_{if} \propto |< \psi_f \mid \Delta \mid \psi_i >|^2 \, \delta(E_f - E_i - h\nu) \tag{2.2}$$

where $|< \psi_f \mid \Delta \mid \psi_i >|^2$ represents the transition matrix element with ψ_i and ψ_f describing the initial and final state wave functions respectively, Δ is the perturbation operator acting on the system and the delta function $\delta(E_f - E_i - h\nu)$ ensures that the total energy is conserved during the excitation process. In the dipole approximation [2] the perturbation operator can be expressed as

$$\Delta = \mathbf{A} \cdot \mathbf{p} \Rightarrow \Delta = \mathbf{e} \cdot \mathbf{p} \tag{2.3}$$

where **A** represents the vector potential associated to the electric field and **p** is the momentum operator of an electron. In case of a linearly polarized light it is convenient to express the perturbation operator as the scalar product between the unit e-vector along the direction of incoming light vector **E** and the momentum operator of the electron.

2.1.1.2 Koopman's theorem and the sudden approximation

One of the first approximations made in order to estimate the binding energy of the level, from which the electron was ejected, is Koopman's theorem [27]. Koopman's theorem relates the kinetic energy of the ejected electron to the binding energy of the level it came from through Eq. (2.1). The electron under perturbation and the remaining system are regarded separately and the perturbation is only acting on the ejected electron. In this case the initial state is the unperturbed N-electron system, whereas the final state consists of the ejected electron and the unchanged (frozen) remaining $(N-1)$-electron system. The solution of the Schrödingers equation for this system, leads to a single final state $E_B = -\varepsilon_k$, where ε_k is the orbital energy of the emitted electron. This would give a single energy in a PE spectrum as indicated in Fig. 2.1 (b, f).

Intuitively it is understood that the remaining $(N-1)$-electron system does 'feel' the changed potential and undergo a relaxation of the levels in order to compensate for the missing electron. This relaxation leads to contraction of atomic levels as well as possible charge transfer in order to minimize the system's energy [27]. Depending on the kinetic energy of the outgoing electron, the relaxation can be either regarded as adiabatic, where the remaining system has the time to adjust to the changes or sudden, where the charge distribution of the system is left at it's initial state. This implies that the final state has to be described as a linear combination of the relaxed eigenstates of the $(N-1)$-electron system, which will usually give several peaks in the photoemission spectrum. The most relaxed state will give the main line in PE spectrum at

[2] Dipole approximation implies that the wavelength of the radiation $\lambda \gg$ x, where x characterizes the size of the excited volume. In case of K-shell excitations, this approximation is satisfied[26].

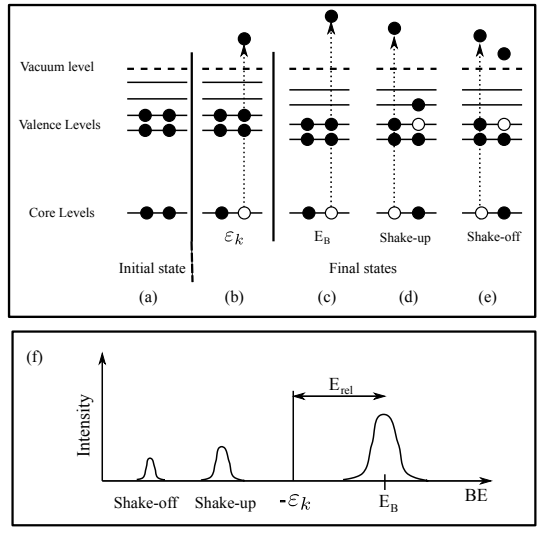

Figure 2.1. A schematic illustration of PES process with electronic levels of the systems in the initial state (a), in a final state after electron excitation to the continuum in a frozen-orbital approximation (b) and in case of a relaxed system (c). Parts (d) and (e) show the shake-up and shake-off processes, respectively. Part (f) is a schematic drawing of the described approximations and mentioned processes on a binding energy scale.

energy $E_B = -\varepsilon_k - E_{rel}$, where E_{rel} is the energy gained by the relaxation of the system. Additional features are produced corresponding to other eigenstates of the $(N-1)$-electron system, which give rise to shake-up and shake-off satellites in the spectra (see Fig. 2.1 (d) and (e)). In these processes another electron is excited to an unoccupied state or to a continuum state, respectively. A schematic drawing of the described approximations from the electronic energy level point of view can be seen in Fig. 2.1 (a)-(e). A schematic drawing of the mentioned processes on a binding energy scale is provided in Fig. 2.1 (f).

2.1.2 Core Levels vs Valence Band

PES studies can be divided into core level (CL) and valence band (VB) studies, which can provide different, but supplementary information about the studied system. Core levels are essentially atomic like levels that do not take part in chemical bonding, thus providing information about the chemical enviroment of a specific atomic site. Nevertheless CLs can be affected by changes in the chemical enviroment of the atom, leading to chemical shifts. Chemical shifts can provide information about the aforementioned change in the chemical surroundings of the atom (change in the geometrical structure, substrate

influence, adsorption, overall charge) as well as indicate the chemical stability of the studied system [28].

The valence electrons on the other hand are situated further away from the center of the atom. Valence electrons can participate in bonding with other atoms and molecules. Due to delocalization and hybridization of the valence levels when new bonds are formed, VB studies ask for a more delicate data interpretation. They can also provide information about the occupied density of states (DOS) of VB and energies associated to different bonds and their involvement in reactions as well as direction of the bonds (polarization dependence to the incoming light) can be determined [29]. Studies in this thesis are mostly concentrated on core level PES.

2.1.3 Analysis of PES

PES data are usually presented as plots of intensity versus binding energy. The analysis of the spectra demands some level of information about the studied system. It can be obtained either from theoretical calculations or general information about the materials under study. In order to obtain information about the chemical shifts or composition of the system, a numerical fit of the experimental data need to be performed. The PE spectrum width is usually influenced by numerous factors. The finite lifetime of a created core hole induces a spectral broadening[3] of a Lorenzian shape. Additionally to lifetime broadening, there are different external factors, such as finite analyser resolution, band width of X-ray source, monochromator, slit resolutions that give additional broadening of a Gaussian shape. Vibrational effects will also broaden the spectra, often with a Gaussian shape. In order to account for all these spectral broadenings, the fitting of PES is done by fitting sets of pseudo-Voigt functions (a convolution of Lorenzian and Gaussian functions) so that the total sum of all functions represents the experimental data. The adjusting parameters include peak position value, peak area and peak width.

Before performing a fit, the background formed by inelastically scattered electrons is removed. There are several types of background functions that could be used, depending on the studied systems. For data presented in this thesis, a *Shirley type* background was used, accounting for inelastically scattered electrons [27].

2.2 X-ray Absorption Spectroscopy

In X-ray absorption spectroscopy (XAS) [4], the photon energy is scanned over an absorption edge of a specific core-level. When the photon energy matches

[3]The values for different lifetime broadenings can be found in literature, e.g [30].

[4]XAS is historically divided into two parts - absorption near edge NEXAFS (Near Edge X-ray Absorption Fine Structure or XANES (X-ray Absorption Near Edge Structure)) which extends

the energy needed to excite an electron, a core-hole is created and the photon is absorbed, exciting an electron to an unoccupied valence level [26]. A spectrum of absorption intensity versus photon energy is obtained, providing information about the unoccupied levels of the atom or molecule. The information can be obtained using different measurement techniques: transmission, total or partial yield measurements, or Auger yield measurements, of which only the last two were used in experiments presented in this thesis.

2.2.1 Principle

XAS probes the unoccupied electronic levels in the presence of the core-hole. The absorption process can be characterized by absorption cross-section (σ_{XAS}), which is defined as the number of electrons excited per unit time over the number of incident photons per unit time per unit area. The absorption probability as in the case of PES, can be expressed by Fermi's 'Golden Rule' (see Sec. 2.1.1) as:

$$\sigma_{XAS} \propto |< f \mid \mathbf{e}\cdot\mathbf{p} \mid i >|^2 \rho_f(E) \tag{2.4}$$

where $\rho_f(E)$ represents the density of states of the unoccupied states, **e** is the polarization unit vector and **p** is the linear momentum operator. The absorption intensity I_{if}, which is measured experimentally, is directly related to the absorption cross-section and only transitions allowed by the dipole approximation [5] will contribute to the intensity. If a linearly polarized light is used, the dipole operator induces an angular dependency of the XA intensity and the orientation of molecules on the surface could be probed.

$$I_{if} \propto |\, \mathbf{e}\cdot\mathbf{O} \,|^2 \propto cos^2\delta \tag{2.5}$$

where δ is the angle bewteen the incoming light polarization unit vector **e** and the direction of the maximum amplitude of some final state orbital **O** [26]. This characteristic is widely used to obtain information about the orientation of the adsorbed molecules on the surface as will be discussed briefly in Sec. 2.2.3.

The created core-hole can be filled by several processes that are schematically shown in Fig.2.2. An electron from a valence level can fill the core-hole and the excess energy can either be emitted as a photon (fluorescent decay) or can cause an Auger decay, whereby an Auger electron is excited into the continuum. For K-shell or low atomic number Z atoms, which is true for species presented in this study, the decay process is dominated by Auger decay [26].

---

to around 50 eV after absoprtion edge and EXAFS (Extended X-ray Absorption Fine Structure) extending up to several hundreds eV after the absorption edge.

[5] Dipole allowed transitions are transitions, where $\Delta l = \pm 1$, l representing the orbital angular momentum.

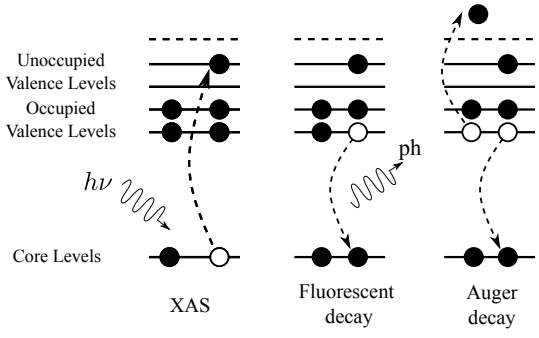

Figure 2.2. A schematic illustration of an X-ray absorption process (XAS) and two possible decay processes - fluorescent decay, where a photon is emitted and Auger decay, where an Auger electron is emitted.

2.2.2 Acquisition of XAS

The absorption process can be monitored and recorded in several ways. One way is by recording the total current coming from the sample, which would give information about all possible final states and is referred to as the total yield mode. This mode is mostly used for bulk measurements. Modes used for surface sensistive measurements are partial yield, where a retardation voltage is set to filter electrons with small kinetic energies (mostly coming from bulk), or Auger electron yield mode, where the signal from Auger decay is monitored (Auger electrons, having a similar IMFP as photoelectrons, provide more surface sensitivity). The acquisition of data can be performed either using a multi-channel plate detector or a hemispherical electron energy analyser set to record electrons in a certain kinetic energy window corresponding to the chosen Auger transition. In order to account for the fluctuations in intensity of the incoming light, as well as the other experimental conditions and uncertenties, a reference signal is taken from a gold plate situated before the sample. In order to obtain the signal coming only from the adsorbed layer, the measurements are normalized to the signal obtained from the clean substrate.

2.2.3 Molecular orientation

Many molecular orbitals (MOs) have a strong directional character and a strong correlation between the direction of individual MOs and the geometry of the molecules exists. For K-shell XAS the initial state is an *s* type electronic state. The final state, following the dipole selection rule can only be of p symmetry. For a planar molecule hybridization between $s - p_x$ or $s - p_y$ orbitals will give σ type MOs, whereas hybridization of $s - p_z$ will lead to a π type MO. In organic molecules like phthalocyanines the π and σ orbitals are oriented in orthogonal directions, providing means to determine the orientation of the molecules on surfaces by comparing the relative intensities of π and σ contri-

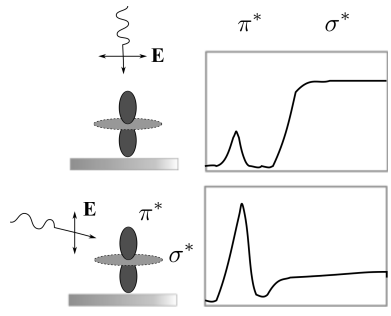

Figure 2.3. An illustration of angular dependency of absorption intensity. The intensity of the signal is dependent on the angle between the **E** vector of the incoming light and the direction of the appropriate p orbital. π^* is represented by a dumbell and σ^* by a circle.

butions in XAS for different orientations of **E** (see Fig. 2.3). Taking absorption spectra for several angles can provide information about the orientation of the molecules on the surface [26].

2.3 Synchrotron based PE studies

From a historical point of view the first X-ray sources used to carry out photoelectron spectroscopy studies were either gas discharge lamps or X-ray tubes. However, with the growth in number and accessibility of synchrotron facilities in the last decades, the latter have gained a significant share of the field. Synchrotron radiation is produced when electrons, travelling at relativistic speed, are radially accelerated by an applied magnetic field. The emitted light has a wide spectral range, high intensity and is strongly focused in a forward direction with a very small angular distribution.

Electrons are accelerated in an injector and afterwards injected into a storage ring, where they travel on a polyhedral trajectory consisting of both straight and bending sections. Synchrotron radiation is produced both on bending (dipole) magnets and also in the straight sections by devices called undulators and wigglers, both of which are constructed from arrays of magnets of alternating polarity and used to oscillate the electrons travelling through the storage ring.

The synchrotron radiation is guided towards the beamlines, where it by a combination of mirror systems is delivered to the sample. Each beamline is equipped with a monochromator that allows the user to set the appropriate photon energy and set other necessary parameters to obtain the desired resolution.

The design of synchrotron radiation equipement is a whole science in itself and will not be discussed in more detail here, but the reader, if interested, is encouraged to view the literature written in the recent years on the subject

[31, 32]. In this thesis, synchrotron radiation has been used as a source of photons with tuneable energy and linear polarization of the incoming light in order to perform surface sensitive PES and XAS experiments.

The studies carried out in this thesis were performed on the I511 and D1011 beamlines of the MAX-lab synchrotron facility in Lund, Sweden, on the Tempo beamline at the Soleil synchrotron in Paris, France, as well as on the GasPhase beamline of the Elettra synchrotron in Trieste, Italy. Detailed description of the beamlines will be discussed in Sec. 4.4.

2.4 Scanning Tunneling Microscopy

Scanning tunneling microscopy (STM) is a technique that probes real space images of sample surfaces with atomic resolution. The inventors - Binnig and Rohrer - obtained the first atomic resolution image of Si(111)7×7 surface in 1983 [33] and since then STM has proven to be one of the best techniques for studying surface structures at the atomic scale. In STM, an atomically sharp tip is scanned over a sample surface at a distance of a few Å. A bias applied between the tip and the surface allows electrons to tunnel between the tip and the sample surface, providing information about the electronic states at the surface. Since the tunnelling is exponentially proportional to the distance between the tip and the sample, it is possible to obtain surface images with atomic resolution.

2.4.1 Quantum tunneling

Quantum mechanical tunneling allows particles (electrons in case of STM) to travel through a vacuum barrier between the tip and the surface. It is possible if the distance between the tip and the sample is small enough so that the extensions of the wave functions of the tip and the sample extending in the vacuum have sufficient overlap (see Fig. 2.4 a)). If a bias voltage is applied to the system, the misalignment of the Fermi levels causes tunneling between the tip and sample. The tunnelling current i_{tunnel} can be expressed as:

$$i_{tunnel} \propto e^{-2\frac{\sqrt{2m\phi}}{\hbar}d}$$

where d represents the distance between the tip and sample surface, ϕ is the average work function of the tip and the sample and m is the mass of a free electron. Since the tunneling current is exponentially dependent on the variations in the z direction (e.g. the height above the surface), in order to obtain atomic resolution, high accuracy in z movements need to be obtained (better than 0.1 Å). Motion is done using piezoelectric elements, which can change their dimensions in the order of an Å when a bias voltage is applied, providing a fine positioning of the tip with respect to the sample surface. Additionally,

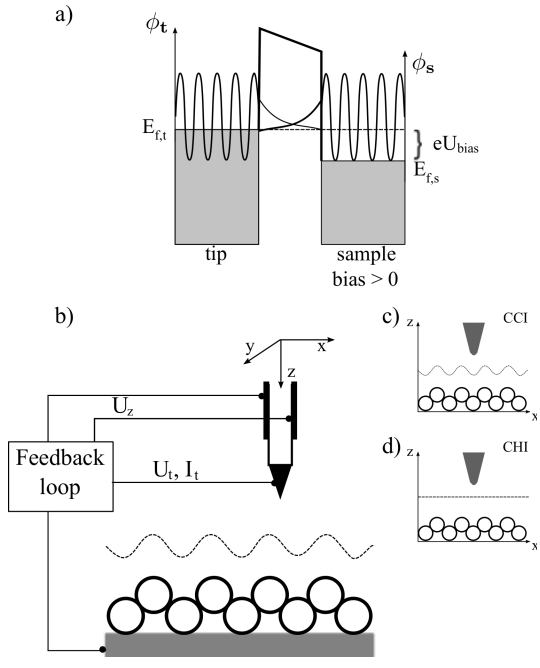

Figure 2.4. a) A schematic illustration of the tunneling event between tip and sample. Filled areas show occupied DOS and barrier heights ϕ_s and ϕ_t are indicated, positive bias of eU_{bias} is applied to sample and electrons tunnel from tip to sample probing the empty DOS of sample; b) A schematic figure of the STM, c) principle of constant current imaging mode, d) principle of constant height imagine mode.

other factors like vibrations (internal or external) need to be minimized, which can be achieved by proper damping of the apparatus and feedback loops in the piezoelectric elements.

2.4.2 Operating principle and imaging modes

A schematic picture of the STM operating principle is shown in Fig. 2.4 (b). The tip is scanned over the sample with the help of piezoelectric elements. In the constant current imaging (CCI, Fig. 2.4 c)) mode the tunneling current is kept constant between the tip and the sample surface. The change in height (z direction here) of the tip is corrected through a feedback loop that sets the appropriate voltage U_z on the piezoelectric element while the (x,y) position of the tip is determined by the values of voltages U_x and U_y. The image of the surface is obtained by transforming the voltage readings $U_z(U_x,U_y)$ into a topography $z(x,y)$. If the constant height imaging (CHI, Fig. 2.4 d)) mode is used, the tip position is kept constant and one obtains the image from the variations of tunneling current $I_t(U_x,U_y)$. Depending on the bias applied on the tip or sample, it is possible to tunnel electrons from either tip to sample or

sample to tip, probing either the occupied DOS or the empty states next to the Fermi level of the sample, respectively.

3. Density Functional Theory

It is common practice and in some cases necessary to combine experimental and theoretical analyses in order to be able to better describe the studied system. Quantum mechanical based modelling methods, like Hartree-Fock (HF) and density functional theory (DFT), together with advances in computer technology have greatly improved the use of simulations to study atoms, molecules and condensed matter in general. It is presently possible to compute relatively large systems at a resonable computational cost. The quantum mechanical methods require solving the Schrödinger equation, which is a prohibitively complex task for multi particle systems and therefore methods based on different types of approximations (HF, DFT) have been developed. In a very simple explanation, DFT works by taking a 3N (N being the number of particles) problem and transforms it in to a 3 variable problem, where the ground state of the system is determined by the electron density $\rho(\mathbf{r})$, where $\mathbf{r}$ represents electron coordinates. Instead of determining the coordinates of the multi-particle system by finding the wave functions of the ground states (done by solving Schrödinger's equations), a different concept is used. It has been proven (Hohenberg-Kohn theorems, Khon-Sham equations[34, 35]) that it is possible to obtain the exact electronic structure of the system by knowing its electron density $\rho(\mathbf{r})$. In practice however, the $\rho(\mathbf{r})$ is approximated by using some density functionals[1] that describe the electron interactions within the system[36].

The ground state calculations and geometry of optimized structure of single molecules of H_2Pc, FePc and $LuPc_2$ as well as H_2Pc and $LuPc_2$molecules on a gold (111) surface were performed by means of DFT. DFT calculations of a single molecule, describing the photoabsorption process were performed using a transition potential approach, where the electronic structure is calculated with a core hole of a fractional occupancy, leading to a properly relaxed valence state. The polarization resolved absorption spectra were simulated for partial density of states (pDOS) of unoccupied *p*-orbitals of both chemically non-equivalent nitrogen atoms and in order to compare to the experimental results pDOS was convoluted with Gaussian curves. Theoretical simulations were adjusted in energy scale relative to the experimental values in order to account for the energy difference caused by the experimental conditions (work function of the sample/analyser are not taken into account for single molecule simulations).

[1] A functional is a function of a function. In DFT the functionals are based on electron density $\rho(\mathbf{r})$ which itself is a function of coordinates $\mathbf{r}$.

4. Experimental

This section describes the samples, their preparation procedures as well as the experimental instruments used to characterize them.

4.1 From 'real world' to model-system and back

The far ahead goal of the current research presented in this thesis is to be able to improve design and efficiency of a sensor device that would work at ambient conditions. However, doing experiments with 'real' devices under 'real'[1] conditions can end up being a tedious exercise with no clear or satisfying outcome, since there are often a large number of parameters that must be considered and measured in order to completely characterize the system and its dynamics. This is where model systems become handy. They allow to tune parameters (nature of substrate, structure, temperature, pressure, ..), making the study more controllable and easier to analyse. When a certain model system has been characterized, new parameters can be added and gradually one can arrive at the end point, which was actually the point of departure - being able to characterize a prototype device as whole. In studies performed in this thesis the model-system consists of a well characterized substrate of choice - silicon Si(100)2×1 or gold Au(111)$\sqrt{3}\times22$ and adsorbants under study - phthalocyanines. All the experiments were performed under ultra-high vacuum conditions.

4.2 The 'Ultra-High-Vacuum' world

Experiments performed in this thesis have been carried out in ultra-high-vacuum (UHV) conditions, which means that samples were prepared and measured in pressure around 10^{-10}mbar. The pumping system (roughing, turbo, ion, Ti sublimation pumps) together with a thorough 'bake-out'[2] can provide a vacuum in order of 10^{-10}-10^{-11}mbar, in which a sample's surface can remain clean for several hours. These kind of experiments demand delicate instrumentation, where different stages of sample preparation and experimental analyses are carried out in an interconnected chamber system, providing sample transfer between them without breaking the vacuum.

[1] Ambient, atmospheric conditions that we are living in.

[2] A process by which the whole instrument is heated up to more than 100°C in order to desorb and pump out molecules from chamber walls.

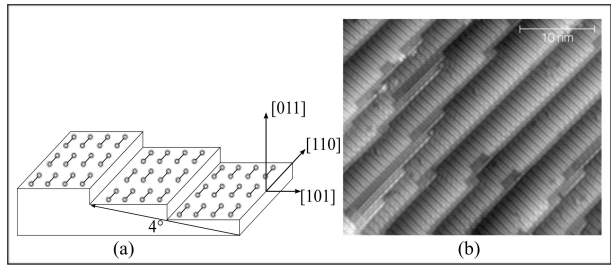

Figure 4.1. Schematic drawing of silicon Si(100)2×1 reconstructed vicinal surface (a) and its STM image (b).

4.3 Samples

The studies presented in this thesis can be divided in two parts. The main focus in this thesis is on phthalocyanine on surfaces, therefore first we present studies performed on model systems that involve Pc molecules adsorbed on certain substrate of choice (Papers I, II, III and IV). The second part of the thesis includes instead two papers about phthalocyanine molecules in gas phase Papers V and VI. The experiments were performed on molecules evaporated and measured in UHV conditions.

4.3.1 Substrates

The substrates chosen for the experiments were silicon, Si(100), vicinal surface, either hydrogen passivated or pristine, and gold, Au(111), surfaces. Both, silicon and gold are materials widely utilized in current electronic devices. However these materials have very different electronic structures. Si(100)2×1 reconstructed surface is a highly reactive material, however when passivated it becomes inert. One gets then the possibility to study the interaction of the molecules and of the molecule-surface interaction on semiconductive and on conductive metal substrate.

4.3.1.1 Si(100) substrate

The Si(100) surface is one of the most widely studied semiconducting surfaces. When a Si crystal is cut in a [001] direction, each surface atom is left with two dangling bonds, however the surface undergoes a surface reconstruction forming 2×1 unit cell (so called dimers), where each surface atom now has only one dangling bond and the surface energy is minimized. Having one dangling bond per atom, the surface remains highly reactive. In order to minimize the reactivity of the surface, the dangling bonds can be 'passivated' using different adatoms, of which the simplest is using hydrogen atoms (this is the species used in this thesis). If a crystal is cut at an angle (larger than 1.5°) with respect to [110] direction, a single-domain stepped surface is obtained, where the dimers are oriented in the same direction (see Fig. 4.1)[37]. One

can therefore distinguish between a single domain (all dimers on a double step surface oriented perpendicular to step edges) and a bi-domain (direction of dimers on successive single steps change from perpendicular-to to paralel-to the step edges) surfaces.

The substrates used in this thesis were cut from a vicinal n-doped Si(100) wafer (Siltronix, France) miscut by 4° in the [110] direction, giving terraces of 3-4nm width, which is roughly the size of the phthalocyanine molecule.

The preparation of the Si substrate is performed in UHV conditions. Prior to introducing a sample to UHV, it is cleaned in an ultra-sonic bath in acetone and ethanol solutions to remove possible organic contamination. After that, the sample is placed in UHV and outgassed for about 12h at a temperature of 600°C in order to get rid of possible contaminants (water, carbon, nitrogen, remnants of cleaning solvents) while still keeping the native oxide layer, which is flashed off at temperatures exceeding 800°C. Then the sample is heated up to 1050°C for 20 second cycles until the pressure stays within the 10^{-10}mbar range during the heating process. Hence, a clean Si surface is obtained. To obtain a passivated surface, a hydrogenation process is performed on the clean surface. It can be done either using a special apparatus (such as an Atomic Hydrogen Source provided by Omicron) or using a tungsten wire placed close to the surface of the sample and using a flow of hydrogen in the UHV chamber. The hydrogen molecules are cracked (by the hot W wire) near the sample surface that is held at 300°C, and the atomic hydrogen binds to the Si dangling bonds.

4.3.1.2 Au(111) substrate

Gold is an extensively studied material and crystals with different surface planes are available. In this thesis the experiments were performed on a Au(111) single crystal substrate. The gold (111) surface reconstructs in a so called herringbone (denoted $\sqrt{3}\times22$) structure with periodically distributed areas of fcc- and hcp-type stackings separated by soliton walls (see Fig. 4.2) (fcc - face-centered-cubic and hcp -hexagonal-close-packed).

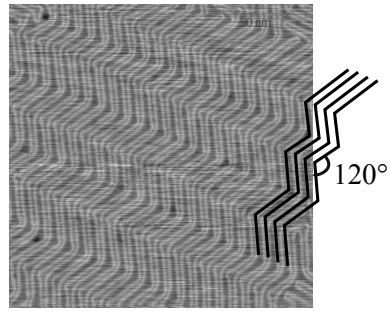

Figure 4.2. STM image of Au(111) herringbone reconstruction. Image shows a 150 nm×150 nm area.

The surface energy is also minimized by forming zig-zag structures with a 120° angle between them [38]. The Au(111) surface was chosen because of its realtively small metallic character (compared to more reactive metal surfaces) and for a comparison with the adsorption on the semiconductive Si(100) surface. The single crystal Au(111) substrate was purchased from Surface Preparation Laboratory (Netherlands). In Paper VI for XPS experiments a gold Au(111)/mica substrate was used. The preparation procedure for gold/mica was the same as for the Au(111) single crystal.

The preparation procedure of a well reconstructed $\sqrt{3}$x22 herringbone structure consists of repeated cycles of argon sputtering and annealing to a temperature of 400°C until the clean surface is obtained.

4.3.2 Phthalocyanines

Phthalocyanines (Pcs) (see Fig. 4.3 (a)-(c)) are planar molecules formed of four isoindole units linked in a circular manner through nitrogen atoms with two hydrogen atoms (a) or a metal atom in the center (b). The chemical for-

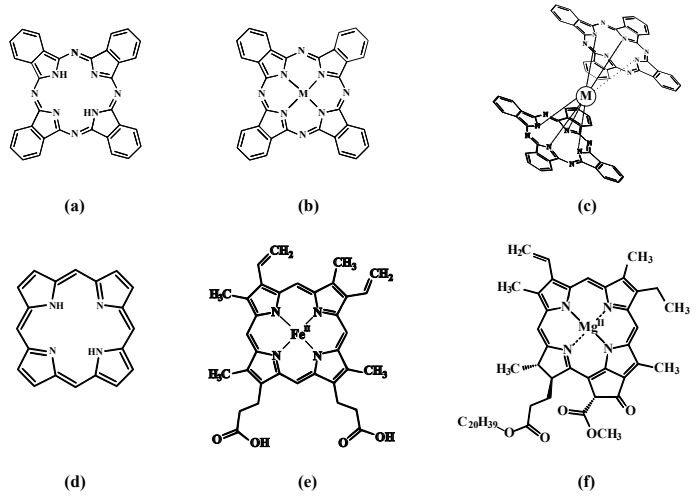

Figure 4.3. Similarities of phthalocyanines to porphyrins and systems in nature. Sketch of H_2Pc (a), MePc (b), $MePc_2$ (c), porphyrin (d), chlorophyll (e) and hemoglobin (f).

mula describing a metal-free phthalocyanine (H_2Pc) is $H_2C_{32}N_8H_{16}$. In the case of metal phthalocyanines the two hydrogen atoms are substituted with the metal atom of choice, giving the formula - $MeC_{32}N_8H_{16}$. Another group of Pcs are so called multi-decker phthalocyanines, having two or more phthalocyanine rings linked together through the metal atoms. There have been numerous studies carried out on different mono-phthalocyanines, whereas much less studies have been performed on double-decker phthalocyanines. The wide

interest in these organic macrocycles is driven by their similarities to biological systems (see Fig. 4.3) - for example - porphyrins (d), found in chlorophyll (e) and in hemoglobin (f). Phthalocyanines have good characteristics, such as high thermal and chemical stability, making them suitable for implementation into different hybrid systems. Their low vapor pressure ($\approx 10^{-14}$mbar) makes them suitable materials to study in UHV conditions.

Film growth. It has been shown that films of Pcs change structures depending on their thickness and, for films above several monolayers, the molecules self-organize themselves in one of the two most common phases - α and β phase (see Fig. 4.4) [39, 40, 41, 42, 43, 44]. Extensive studies have been carried out on phthalocyanine monolayers on different substrates, investigating the influence of the substrate on orientation and on electronic structure of phthalocyanine molecules [3, 45, 46, 47, 48, 49]. These studies show that phthalocyanines prefer the planar adsorption in the first layers and tend to redress themselves in thicker films in one of the two most common phases (α or β phase). Additional studies on different deposition methods (sublimation, Langmuir-Blodgett films) and sample treatment (grain size effects [42], heat treatment [50], solvent vapor treatment [51]) have shown influence on molecular organization. Different stacking of the molecules leads to different properties of the system and by controlling the organization of the molecules, tuning of different properties can be obtained. Specific characteristics of different devices ask for different structures. For example, solar cell application would benefit from well arranged $\pi - \pi$ favoured stacking of the molecules, since the orientation of the column determines the preferential electron (hole) hopping [52]. Whereas organization of molecules parallel to the substrate surface has shown to maximize the efficiency of gas sensor devices[53].

In the work presented in this thesis the main objects of interest were iron phthalocyanine (FePc) and lutetium biphthalocyanine ($LuPc_2$).

Iron phthalocyanine is a mono-phthalocyanine with Fe(II) ion in the central cavity. Particular interest in studying FePc lies in its catalytic capability of oxygen reduction and similarities to the oxygen-binding active centers in hemoglobin (Fig.4.3 (b, f)).

Lutetium biphthalocyanine is a doule-decker phthalocyanine with Lu(III) ion 'sandwiched' between the two Pc rings. Having an unpaired electron in a

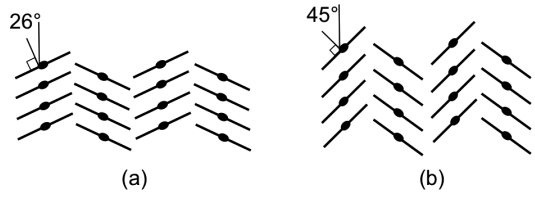

Figure 4.4. Schematic illustration of the α (a) and β (b) phases of phthalocyanines.

semi-occupied molecular orbital, it can be easily reduced or oxidized making it a good candidate for gas sensing applications.

Preparation. The sublimation temperatures vary in the range from 250°C for H_2Pc up to $300° - 400°C$ for $LuPc_2$ and $400° - 470°C$ for FePc. Before each experiment the molecules were outgassed carefully at temperatures slightly below their sublimation temperatures in order to get rid of contaminants remaining from the synthesis process.

4.4 Experiments at synchrotron facilities

The studies presented is the thesis were performed at different synchrotron facilities - on Tempo beamline (BL) at SOLEIL (Paris, France), on the GAsPHase BL at ELETTRA (Trieste, Italy), the I511 (as a surface branch line) and D1011 BLs at Max-Lab (Lund, Sweden).

GAsPHase is an undulator based BL, which is constructed in such a way to allow performance of gas phase measurements at pressures up to 10^{-4}mbar, which is regulated by differential pumping systems[54]. The incoming photon energy range spans between 13-900 eV. Beamline I511 (construction before 2011) and D1011 both are beamlines suited for surface physics experiments. I511 is an undulator based BL with a plane grating monochromator providing high-intensity linearly polarized synchrotron radiation of photon energies ranging from 100 to 1500 eV. The end station was equipped with hemispherical electron energy analyzer rotatable around the incoming beam suitable for surface sensitive measurements [55]. In 2011, the I511 end-station was rebuilt as a high-pressure soft x-ray BL [56] allowing to perform measurements in gaseous atmospheres up to near-ambient pressures (up to a few mbar). A typical BL end-station dedicated for surface science measurements (such as D1011, I511) is equipped with instruments for surface preparations, such as the possibility to heat the sample, a sputtering gun with a dedicated gas-inlet system, a low-energy electron difraction (LEED) instrument to check the surface reconstruction and additional ports for user required instruments like molecular evaporators as in our case. The high-pressure BL is a good example of 'reducing' the gap between UHV and ambient pressure experiments, which allows one to get information on systems closer to 'real world' conditions, while still not complicating the experimental conditions too much.

4.5 Energy calibration of XPS and XAS spectra

The energy calibration of the PES was performed adjusting the BE scale of experimental spectra to a characteristic signal of the appropriate substrate. In experiments performed on a gold substrate (Paper III and Paper IV), the calibration was done by adjusting the spectra of C 1s, N1s to the energy position

of the Fermi edge of gold substrate which was taken under the same experimental set-up (photon energy, electron and photon resolution) as the measured core-level photoelectron spectra.

In the case of experiments performed on a silicon substrate (Paper I and Paper II), the BE scales of C 1s and N 1s were calibrated with respect to Si 2p peak BE (99.35 eV, value taken from [57], taken at the same photon energy and same resolution as the measured core-level photoelectron spectra.

In the case of gas phase experiments, the calibration of the BE scale was performed by introducing gases into the chamber giving an XPS peak of known binding energy as reference. Different gases are used for calibration of different binding energy regions.

Calibration for XAS measurements performed in partial (or Auger) electron yield mode is done by calibrating the photon energy window of the specific absorption line. The calibration is performed by taking the PES spectra of some intense line (C 1s, Si 2p or Au 4f) with 1st and 2nd order light. Then the difference in kinetic energies between 1st and 2nd order light should be equal to the set photon energy.

4.6 Thickness estimations

Estimation of adlayer thickness for STM and PES studies turns out to be a complicated task. One of the easiest ways would be to use a quartz balance to estimate the amount of evaporated molecules in a given time, however this is not always possible due to the limitations for the experimental set-ups. Therefore, other thickness estimation techniques need to be used. In our PES measurements the thickness was estimated using a so-called overlayer method, where the thickness of the sample can be estimated from the relation between the photoelectron intensity of the photoelectron line and the inelastic mean free path (IMFP) of the detected photoelectrons:

$$I_s = I_s^0 exp(-d/\lambda_s cos\Theta)$$

where I_s^0 is the intensity of PE line from the clean surface, I_s is the intensity of the same peak through the overlayer, d is the thickness of the overlayer, λ_s is the inelastic mean free path, Θ is the angle between the electron detection direction and surface normal, which in our case was 0°. The kinetic energy independent IMFP was estimated using the formula proposed by Tanuma et al. [58]. This thickness calculation can give a good estimate of the overlayer thickness, but has to be considered with caution since in the formula a homogeneous overlayer is assumed, which is not the case for phthalocyanine films on semiconductor surfaces.

4.7 Scanning tunneling microscopy

STM experiments performed in this thesis were performed at the Institut de Nano-science de Paris (UPMC, France) on a commercial Enviromental Omicron instrument. The instrument consisted of two inter-connected UHV chambers - a preparation chamber and the STM chamber. The preparation chamber was equipped with a LEED instrument for surface analyses, sputter gun and sample heating unit for surface cleaning as well as the molecular evaporator and the atomic hydrogen cracker units. A load-lock entry was connected to prep-chamber to allow an easy sample introduction into the UHV system. The STM system was cooled down to 95K using liquid nitrogen. Self prepared tungsten tips were used for the measurement. Since a good tip is one of the most important requirements to obtain an atomically well resolved STM image, particular care was paid to the preparation of the tips. The tungsten wire (first cleaned in an acetone, then in an ethanol ultrasonic bath) was electrochemically etched in a NaOH solution ($\approx$ 2mol/L) in order to obtain an atomically sharp tip. After insertion in UHV, it was heated to around 800°C in order to eliminate the oxide layer of the tip.

5. Summary of Papers

This chapter is dedicated to the summary of the work presented in this thesis and is structured following the different studied systems, first discussing phthalocyanines on different surfaces, followed by discussions on gas phase studies of phthalocyanines.

5.1 Adlayers of phthalocyanines on surfaces

Papers I-IV present studies of different phthalocyanines on either Si(100)-2×1 or Au(111)$\sqrt{3} \times 22$ surfaces.

5.1.1 $LuPc_2$ on Si(100)-2×1 surface

In Paper I and Paper II the adsorption of $LuPc_2$ on Si(100)-2×1 surfaces is investigated. We have compared the adsorption on passivated Si(100)-2×1:H surface and pristine Si(100)-2×1 surface and observed differences in the molecular adsorption geometries as well as in the molecular electronic structure.

5.1.1.1 $LuPc_2$ on passivated Si(100)-2×1 surface

In Paper I we show the evolution of adsorbed layers of $LuPc_2$ on Si(100)-2×1:H. The PE spectra of C 1s, N 1s, as well as Si 2p were recorded in order to follow the evolution of the lines upon increasing the adlayer thickness. The low coverage data show (see Fig.3 in Paper I) no noticeable interaction between the substrate and the $LuPc_2$ molecules and the PE spectra are similar to those of a molecular film.

The XAS studies of N K edge were carried out on samples with different thickness of $LuPc_2$. The results reveal a change in the average orientation of the molecular plane with increasing thickness. Comparison between the relative intensities of $\pi^\star$ and $\sigma^\star$ resonances, show that at monolayer coverage the molecules adsorb with the molecular plane parallel to the surface and, with increasing thickness, they tilt reaching an average angle of about 45° from the surface. The DFT single-molecule calculations for $LuPc_2$ provide an insight into the origins of different features observed in the XA spectra (see Fig. 5.1, left) as well as information about the charge densities of the ground state (Fig. 5.1, right side). The theoretical calculations at two orthogonal directions of polarization vector of the incoming light are presented on

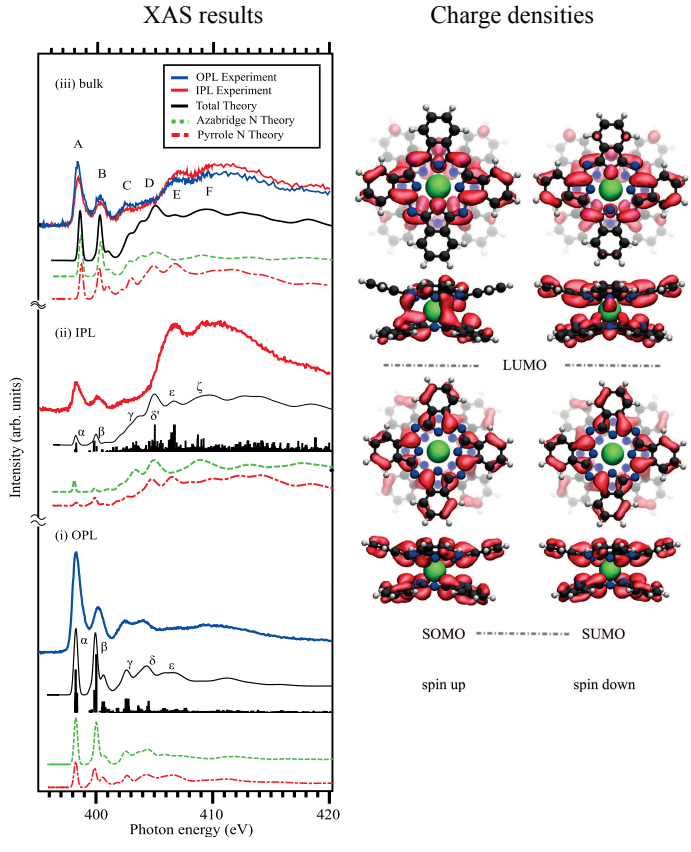

Figure 5.1. Experimental and theoretical XAS (left side) and picture of charge densities obtained from the ground state calculations for SOMO/SUMO and LUMO (right side). (i) $\pi^\star$ resolved calculation and measurement for $E_\perp$ (OPL) polarization of a 0.3 nm thick film, (ii) $\sigma^\star$ resolved calculation and measurement of $E_\parallel$ (IPL) polarization of a 0.3 nm thick film, (iii) calculation for $\theta = 45^\circ$ composed of $\pi^\star$ and $\sigma^\star$ calculation compared to bulk measurements. Figure taken from Paper I.

left side graph in Fig. 5.1. An experimental result from 0.3 nm thick film (i-ii) is presented together with the theoretical calculations. The DFT calculations for single molecule are in very good agreement with experimentally obtained spectra and provide information about the atomic origins of each structure (pDOS). All the XA spectra include peaks labelled with letters from A-F (Fig. 5.1, left). The spectrum which is dominated by the $\pi^\star$ resonances (OPL) is shown in Fig. 5.1(i). The theoretical calculations of pDOS show how both pyrrole and aza-bridge nitrogen atoms contribute to the intensities of this XA spectrum.

Slightly different situation is observed for the spectrum taken in the other geometry (IPL), showing mainly $\sigma^\star$ intensity (Fig. 5.1 (ii)). The two peaks at lower photon energies (A at 398 eV, B at 400 eV) get each different con-

tributions from aza-bridge (A) and pyrrole (B) nitrogens. It is interesting to point out that also the theoretical calculations show intensities in peaks A and B for IPL geometry despite the orientation of the molecule. These features are observed only for metal phthalocyanines and originate from the bonds formed between the orbitals of nitrogen atoms and the central metal atom. The $\sigma^\star$ resonance intensity, above 406 eV is formed from N 1s electron transitions to empty σ states from both types of nitrogen atoms.

However, in case of the thick layer (Fig. 5.1,(iii)) the contribution to the intensity at the threshold region comes also from the transitions to the π states due to the orientation of the molecules not completely parallel to the surface. In fact, in Fig. 5.1 (iii) the experimental spectra for thick samples are in very good agreement with the shown DFT calculations for molecule adsorbed at 45° angle with respect to the surface.

5.1.1.2 $LuPc_2$ on pristine Si(100)-2×1 surface

In Paper II the evolution of the molecular organization of $LuPc_2$ on pristine vicinal Si(100)-2×1 surface is presented and compared with the results presented in Paper I. Samples of different thicknesses, ranging from 0.3 nm up to 4.4 nm, were studied using PES and XAS. The molecular orientation was imaged using STM for submonolayer thickness.

In Fig. 5.2 C 1s and N 1s spectra for different adlayer thickness of $LuPc_2$ are shown (a-c). It is possible to observe that the PE C 1s and N 1s peaks shift to lower binding energies with increasing thickness (see Fig.2 in Paper II). The peak position for thick layers are found at the same BE as for $LuPc_2$ film on passivated Si surface. The observed shift in BE can be an effect of both initial and final states. Determining the exact reason is not a straight forward task usually involving theoretical calculation. The observed broadening of the C 1s and the N 1s spectra (a) can be ascribed to intensity coming from several energetically different adsorption sites. For this reason, the XP spectra have been fitted with two sets of peaks shifted in energy and representing the intensities from the different adsorption sites. The spectra (d) of a thick layer of $LuPc_2$ on passivated Si, representing a non-interacting system, has been used in the fitting of C 1s and N 1s spectra at low coverages. However, both the change in line shape and the BE shift for PE spectra at low coverages, can be ascribed to the interaction of $LuPc_2$ with the pristine Si surface.

The hypothesis of two adsorption sites is further strengthened by the STM images on submonolayer coverage samples (see Fig. 5.3). Figure 5.3 shows a STM image of $LuPc_2$ on pristine Si surface. Two different adsorption geometries can be identified, marked either **I** or **II**. Type **I** molecules have a 4-fold double lobe structure, typical for double-decker phthalocyanines, whereas type **II** molecules appear as squares and have two distinct brighter protrusions either along the dimer rows or in between dimer columns of the underlying Si surface. The difference in height, measured by STM, in agreement with expected thickness of the $LuPc_2$ molecule, allowed us to exclude the dissociation

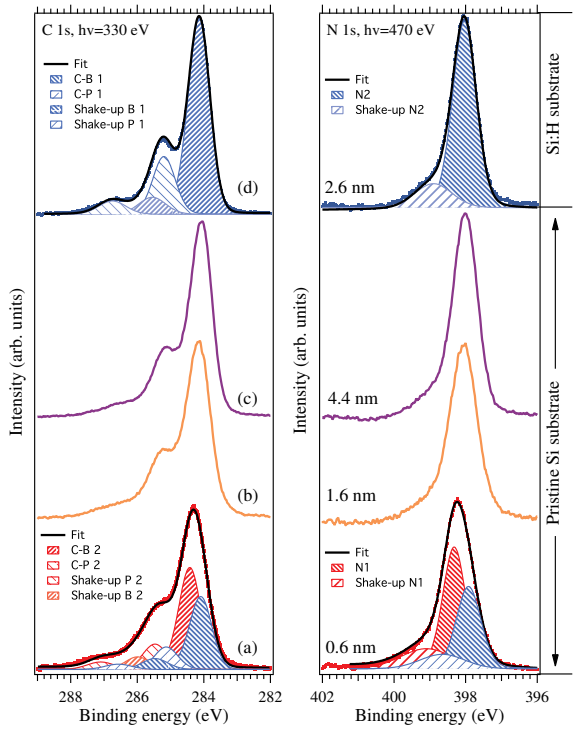

Figure 5.2. XPS C 1s and N 1s spectra for pristine Si samples with different thicknesses (a-c) compared to passivated Si:H sample (d). Thicknesses of the adlayers are indicated in the N 1s graph (right graph). Fitting components are shown in blue and red. Figure taken from Paper II

of the double-decker and type **II** molecules just being monophthalocyanines. Linking both the STM and the PES results, we propose two energetically different adsorption geometries, where type **I** molecules have a very weak interaction with the pristine Si, whereas type **II** molecules have a much stronger interaction leading to BE peak shift to higher BE and possible charge redistribution between the Si substrate and molecule.

The XAS studies performed on layers of different thicknesses showed a much more disordered molecular organization that on passivated Si substrate presented in Paper I. Furthermore, the XAS results indicate a non-negligible interaction between the molecules and the surface at low coverages However more studies are needed to provide a more detailed description of the interaction.

5.1.2 $LuPc_2$ on Au(111) surface

Paper IV presents a study of $LuPc_2$ on Au(111) surface, where the main attention is pointed at the molecular orientation characterized by STM mea-

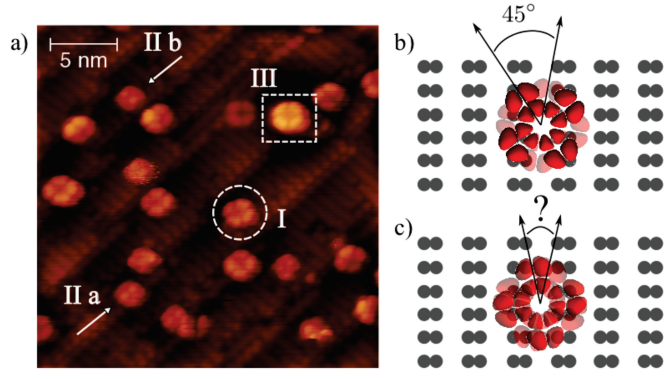

Figure 5.3. STM image of $LuPc_2$ on vicinal Si. (a): Image taken with bias voltage -2V on the sample, tunneling current I=50 pA, image size 25nm x 25nm. Different molecular orientations and adsorption geometries are pointed out. Example of type I molecule is shown with a white circle (I). Example of type II molecules are ponted out with arrows (II a and II b). A white square (III) shows a $LuPc_2$ on top of another molecule. (b) and (c) presents a sketch of the proposed adsorption geometries of type I and type II moelcuels, respectively. Figure taken from Paper II.

surements. A comparison between the adsorption sites and orientation of the molecules between the 'as-evaporated' layers and the annealed layers are shown. In Fig. 5.4 STM images on large scale image (A) and a smaller scale image (B) are shown with the indication of height profile of the layers formed on the surface. In this study we have seen that $LuPc_2$ molecules adsorb in bi-layers starting from the submonolayer coverage (see for example Fig.3 in Paper IV) and remain in bi-layer formation also upon annealing for several minutes at 280°C (Fig. 5.4). There are two identified domains where molecules are arranged in square lattices with an angle of 44° between the two domains. This study can be considered still as preliminary and more measurements need to be carried out for a thorough characterization of the system.

5.1.3 H_2Pc on Au(111) surface

Metal-free phthalocyanines are the simplest molecules within the Phthalocynanine family. It is very easy to distinguish the H_2Pc from any other metal Pc molecule by PES. H_2Pc molecule is formed of two hydrogen atoms occupying the central cavity, resulting in total of three nitrogen species, which have a different chemical enviroment, resulting in two separable features in PE N 1s spectra (Fig. 5.5, a). For metal Pcs the N 1s spectrum is instead formed by only one broad feature, since metal Pc molecules have only two chemically different N atoms. Therefore this characteristic allows us to easily distinguish

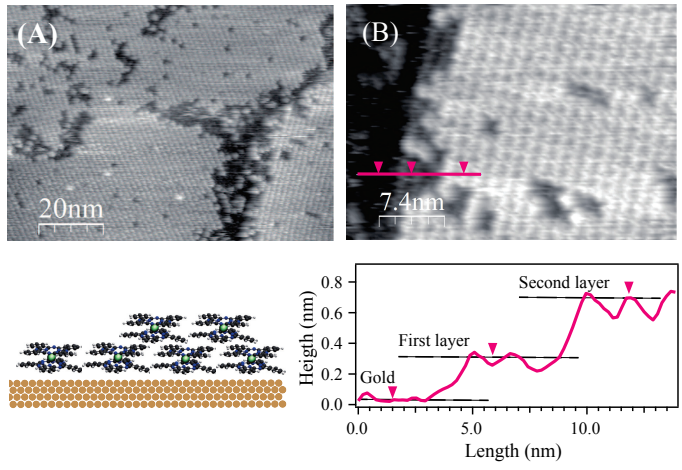

Figure 5.4. STM image of $LuPc_2$ on Au(111) surface after annealing: (A) 100 nmx85 nm, V=-0.8V; (B) 37.1 nmx26.6 nm, V=-0.8V; corresponding line profile is plotted below the image together with a sketch of proposed molecular arrangement. Figure taken from Paper IV.

H_2Pc from any metal Pc, considering the N 1s line profile in PES (see Fig. 5.5, b).

In Paper III we show a PES and XAS study of the multilayer and the monolayer of H_2Pc on Au(111) ($\sqrt{3}x22$) surface. The comparison between the monolayer and the multilayer of H_2Pc indicates a noticeable interaction between H_2Pc molecules and gold surface at monolayer coverage. A surface induced shift of both C 1s and N 1s peaks to higher BE (see Fig. 2 and 3 in PaperIII) is observed at increasing molecular coverages. This is attributed to a different core-hole screening in the monolayer with respect to the multilayer. The monolayer spectra is noticeably broadened, if compared to multilayer spectra, explained by the migration of molecules to different adsorption sites upon the sample preparation i.e. annealing of the multilayer.

The XA spectra of N K edge for multilayer and monolayer are shown in Fig. 5.6. The spectra are taken at two almost orthogonal directions of polarization vector **E** of the incoming light. By comparing the relative intensities of $\pi^\star$ and $\sigma^\star$ contributions (see Sec. 2.2.3), we found that the molecules lie flat on the surface from the first layer and keep the same orientation also for thick layers.

However, an interesting observation regarding the lower photon energy region is seen for spectra taken with in-plane polarization of the incoming light vector (IPP, $E_{||}$). Both spectra contain two features at lower photon energies, however, their relative intensities and relative energy positions are different for multilayer and for monolayer. The theoretical calculations performed on a single molecule on Au(111) cluster, allowed us to obtain information about

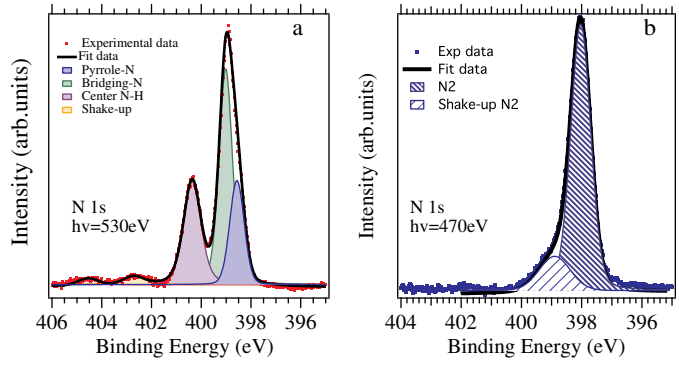

Figure 5.5. Comparison between the N 1s (a,b) spectra for H_2Pc and $LuPc_2$ thick layers. Spectra taken from Paper III (a) and Paper II (b).

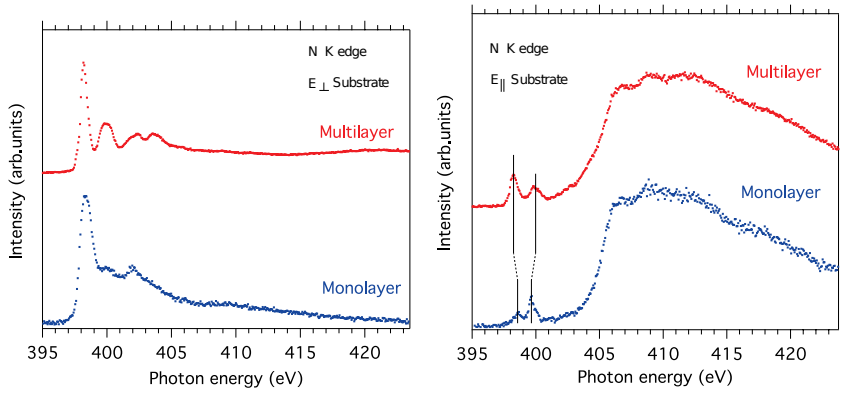

Figure 5.6. XA spectra of N K edge for H_2Pc multilayer (top) and monolayer (bottom) on Au(111) substrate taken in two different directions of polarization vector with respect to the sample surface. Figure taken from Paper III.

the different contributions to the N 1s XA spectra (see Fig. 5 and Fig. 6 in Paper III). The first peak at 398.2 eV in out-of-plane polarization (OPP, $E_\perp$) is formed from excitations into the empty π orbitals from aza-bridge and pyrrole nitrogen atoms, whereas the second peak at 400 eV get contributions from all the nitrogen atoms. In $E_\parallel$ polarization there is a small contribution to the first peak at 398.5 eV from the aza-bridge nitrogens and a broad feature at higher photon energies corresponding to the σ states and having contributions from all types on nitrogen atoms. The threshold features in the multilayer sample taken with $E_\parallel$ is ascribed to a possible tilt angle between the molecular plane and sample surface, leading to a projection of some π orbitals. This is consistent with previously performed studies on other types of Pc molecules on surfaces, where a tendency of change in the angle of the molecular plane

of the molecule with respect to the surface has been observed for increasing depositions [59].

However, for the monolayer spectrum, this would not explain the change in the relative intensities between the two $\pi^\star$ features. The change in the energy position as well as in the relative intensity could be the result of the combination of several effects. Since the peak intensities in the XA spectra are linked to the occupancy of the orbitals into which the core electrons are excited, a change in intensity between multilayer and monolayer spectra could be induced by the adsorbate-substrate interaction (charge transfer between the substrate to the molecule). The change in energy position could also be caused by interaction and hybridization with the substrate and then formation of new hybrid states.

5.2 Gas phase experiments

In Paper V, a study of gas phase of FePc has been presented. Gas phase studies in general provide information about the electronic structure of pure molecules or atoms. However, for us, working in surface science, such studies are important since they allow us to investigate the differences induced on such molecules and atoms by external factors, e.g. being adsorbed on different kinds of substrates, evaporation conditions and many more. In Paper V we show gas phase PE spectra of C 1s, N 1s and Fe 2p, as well as XA spectrum of N K edge of FePc. We compare these gas phase results with those obtained when the same molecules were adsorbed on Au(111) and Si(100). A good agreement between the gas phase and thick layer results of FePc indicates that in thick layers the adsorbed molecules retain a molecular-like electronic structure. The Fe 2p core level spectrum, showed in Fig.5.7, consists of two components due to spin-orbit splitting, found at 726.8 eV at 713.5 eV for Fe $2p_{3/2}$ and Fe $2p_{1/2}$, respectively. The agreement between the gas phase results and the thick film shows that the Fe metal retains Fe^{+2} ionic state. This gas phase spectrum can be considered as a 'fingerprint' for the Fe(II)Pc and will serve in monitoring the modifications in the electronic structure of the FePc molecule, when studying such molecular films under different conditions (e.g. high-pressure studies for gas sensing or catalysis).

5.3 Valence band and the influence of the central metal atom in phthalocyanines.

Paper VI presents a comparison of the valence band PE spectra of metal-free and two different metal phthalocyanines. Iron phthalocyanine and manganese phthalocyanine were chosen for this study to compare the influence of different metal atoms on the VB region due to the different occupancy of their

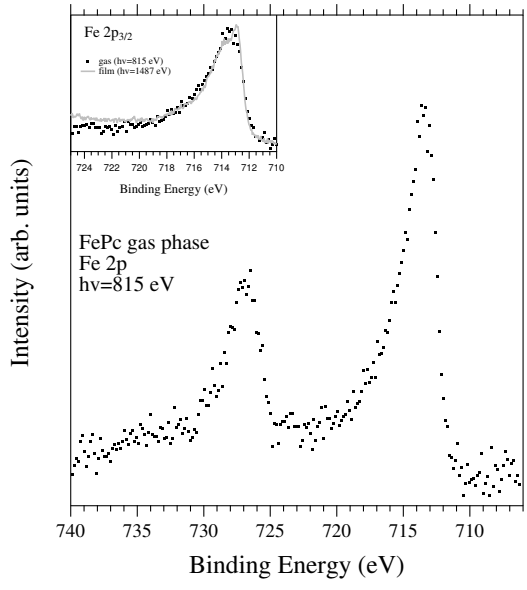

Figure 5.7. Fe 2p photoemission spectrum of FePc gas phase. In the inset a comparison with Fe $2p_{3/2}$ photoemission spectrum of a film of FePc on Au(111) substrate.

3d states. It has been shown that the 3d states are responsible of the molecular magnetic and conduction properties. It is interesting to characterize the differences induced by the metal in the molecular centre, compared to the metal-free phthalocyanine. The experimentally obtained valence PES results are compared with the theoretical single-molecule calculations, allowing to determine the different atomic contributions to the intensity peaks observed in VB spectra. We show that the VB spectra of a metal phthalocyanine cannot be explained by a mere superposition of a metal-free phthalocyanine VB with the respective metal atom contributions.

The partial and total DOS are shown for the three phthalocyanines in Fig. 5.8. It is possible to observe the weight of the different atomic contributions on the total DOS and hence the resulting VB spectra. The molecular structure of a metal phthalocyanine can be seen in Fig. 4.3 or in Fig. 1 of Paper V. The position of metal atom in the central cavity of the Pc ligand results in a stronger influence on the pDOS related to the nitrogen atoms than on the pDOS of the carbon atoms (Fig. 5.8, b-c). This is a quite expected result since the C atoms are situated much further away and are not in the direct contact with the metal atom. The C 2p orbitals are mostly affected for the inner VB regions from 12-25 eV binding energy, whereas for the N 2p orbitals the influence is seen also on the outer VB region above 8 eV BE. The resulting VB electronic structure reveals that in H_2Pc and FePc the HOMO is formed entirely of C 2p orbital contributions, whereas for MnPc the HOMO is formed mostly by Mn 3d states with a slight contribution from C 2p orbitals. The HOMO-1 for H_2Pc is

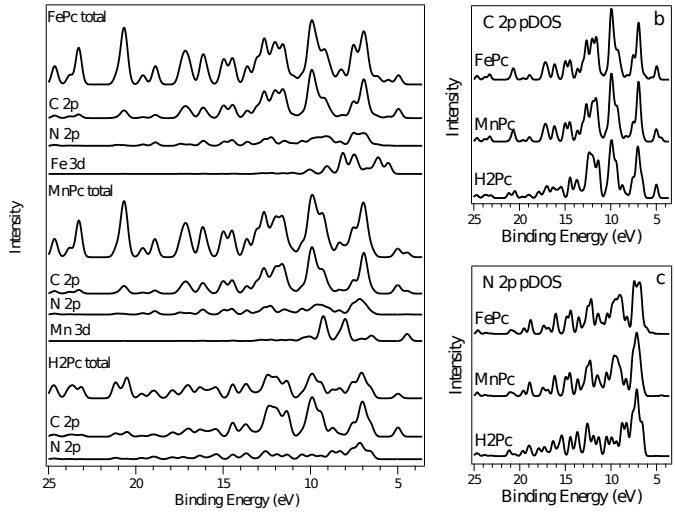

Figure 5.8. DFT calculated atomic partial and total DOS of H_2Pc, FePc and MnPc (a) and C 2p partial DOS (b) and N 2p partial DOS (c).

formed from a combination of C 2p and N 2p orbitals. For FePc the HOMO-1 has mostly Fe 3d character, whereas for MnPc the HOMO-1 is formed from C 2p contributions. In Fig. 5.9 a comparison between the theoretical calculations and the experimental data are shown for all three Pcs for two different photon energies. The DFT calculations represent very well the experimental data and by varying the photon energy, it is possible to follow the photon energy-dependent intensity variations of the VB peaks. The metalic character of the HOMO region is enhanced at higher photon energy (1486.7 eV, a-d) where the cross-section is maximized for metal atoms, whereas for lower photon energy (21.2 eV, b-d) the VB is formed from the enhanced contributions of C 2p and N 2p orbitals.

5.4 Conclusions

The presented studies of phthalocyanines on different surfaces show the complexity of mastering the control of molecular adsorption and substrate induced effects. Nevertheless it is an exciting field with a huge perspective for improvement of molecular and hybrid electronic devices.

The studies based on $LuPc_2$ molecules adsorbed on different surfaces yield interesting conclusions. The studies give insights in the importance of substrate on factors like molecular orientation and electronic structure of the phthalocyanines. The choice of three different substrates from the most inert Si:H to the most reactive pristine Si, have provided the possibility to follow the modifications of the molecular electronic structure and orientation induced by the interaction with the substrate. The least reactive passivated

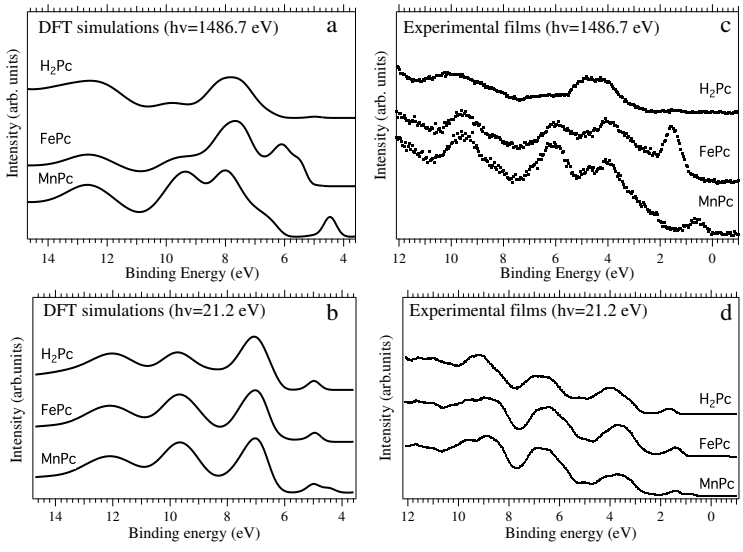

Figure 5.9. a-b: Single molecule DFT simulations of H_2Pc, FePc and MnPc valence photoelectron spectra modified according to the cross-section for excitation energies of 1486.7 eV (Al K_α) and 21.2 eV (He I), respectively. c-d: PE experimental VB results for H_2Pc, FePc and MnPc films on Au(111) for PE of 1486.7 eV(Al K_α) and 21.2 eV (He I), respectively.

Si substrate, provides a well-ordered $LuPc_2$ layers, starting from submonolayer coverages up to thicker layers. The gold substrate shows similar results from the molecule orientation point of view as for Si:H, but additional influence from the substrate is observed for low thicknesses of adsorbates, resulting in BE shift and broadening of spectral peaks. $LuPc_2$ adsorption on pristine Si gives remarkably different results considering the expected significant surface-molecule interaction on such reactive surfaces. The molecules tend to aggregate and form clusters starting from the submonolayer region and due to the clustering from early stage of adsoprtion, the thick layers seem more disordered than on passivated Si and gold substrates. The obtained results show the importance of properly choosing the substrate, since it will have an influence to the electronic structure of the whole system.

We have also characterized the electronic structure of metal Pcs like FePc and MnPc molecules. The understanding of how the outermost orbitals are formed for the different phthalocyanines and the influence of different metal atoms on their electronic structure can be of importance, when specific molecules are chosen for specific applications. Our studies presented in Paper V and Paper VI can be of interest, since they provide the starting point for the characterization of Pc based devices.

6. Summary in Swedish

Ytvetenskap

Denna avhandling studerar molekylernas struktur då de binder till halvledar- och metallytor. Studien handlar om grundläggande egenskaper hos olika modellsystem. Skälet att använda sådana system är att många viktiga processer som involverar atomer och molekyler äger rum på ytor. För att kunna studera specifika växelverkningar måste mycket speciella villkor uppfyllas. Exempelvis måste man begränsa inflytandet från alla andra atomer och molekyler som finns runt omkring. Detta är skälet till att studierna utförs i en så kallad ultrahögvakuum (UHV)-kammare,där man reducerat antalet oönskade molekyler genom att ta bort dem med moderna effektiva vakuumpumpar. Detta begränsar antalet kollisioner mellan de partiklar vi vill studera och andra partiklar och tillåter oss att använda tekniker som i vårt fall innebär detektion av de elektroner som lämnar provet. För att ge en bild av varför det förhåller sig så kan man föreställa sig att man befinner sig på Stockholms Centralstation en jäktig dag före jul för att möta en gammal vän och att man kanske har svårigheter att känna igen honom eftersom man senast sågs för 10 år sedan. Och vännen råkar befinna sig på motsatta sidan av hallen. Det är inte lätt att nå honom eftersom man hela tiden knuffar på folk runtomkring, och dessutom är man inte säker på vem som är den gamle vännen. Emellertid, om du råkar vara där kring midnatt samma dag så är hallen nästan tom och då finns bara några få människor att välja bland. På samma sätt kan experiment utförda på modellsystem i vakuum vara lättare att tolka jämfört med studier vid normalt tryck och temperatur, där omgivningen är fylld med massor av ovidkommande molekyler. De experiment som finns redovisade i denna avhandling är alla utförda under UHV vilket innebär att ganska komplicerade experimentstationer har utnyttjats (bl.a. slutna vakuumkärl som anslutits till varandra för att åstadkomma transport av provet från ett experiment till ett annat). Två experimentella metoder har använts för analyserna: Sveptunnelmikroskopi och fotoelektronspektroskopi. De studerade systemen består av ftalocyaniner som lagts på olika ytor.

Vad är ftalocyaniner och varför är de intressanta att studera?

Ftalocyaniner (Phtalocyanines, Pcs, låt er inte skrämmas av namnet) är plana molekyler som är huvudsakligen uppbyggda av kol- och kväveatomer. Några

av dem har metallatomer mitt i molekylen. Intresset för dessa molekyler har uppstått genom att de uppvisar likheter med system i naturen t.ex. med klorofyll som finns i gröna växter, eller med hemoglobin som finns i våra kroppar. Ett av forskningsspåren idag är att minimera storleken på de system vi utnyttjar för olika syften ända ner till att vi använder oss av en enda molekyl för att åstadkomma en effekt. En sådan molekyl kan då användas för att ersätta en större apparat. Till exempel kan molekyler användas som switchar genom att de ändrar sin form. Alternativt kan vi använda anordningar som härmar de processer som naturen använder, t.ex. funktionen där hemoglobin tar upp syre. För att komma till detta ofta rätt utopiska steg måste vi lära oss reglerna för den atomära världen. Det är ett mycket komplext arbeta att förstå, kontrollera och styra specifika molekyler. Något som kräver intensiv experimentell och teoretisk forskning.

Göra det möjligt att se närbilder av molekyler

En av de avancerade tekniker som använts i denna avhandling är sveptunnelmikroskopi (STM) som gör det möjligt att se bilder av molekyler på ytor. Principen för STM är att man utnyttjar den s.k. tunneleffekten, som är en kvantmekanisk process som möjliggör att en elektron kan förflytta sig från ett material till ett annat, även om det finns en barriär däremellan. Detta kan bara ske om materialen är väldigt nära varandra; i praktiken rör det sig om några ångström. I ett STM-experiment använder man en spets som kan skärpas automatiskt och som sveper över ytan. Man mäter tunnelströmmen och då den är beroende av avståndet mellan provet och spetsen får man en bild som avbildar elektrontillstånden på ytan. Eftersom elektronerna är lokaliserade till olika atomer så kan bilden tolkas som en atomär bild av ytan. I denna avhandling har vi utfört STM mätningar på Lutetium bi-ftalocyaninmolekyler på olika ytor, vilket har gett oss möjlighet att förstå växelverkan mellan molekylerna och substraten. Vi kan också förstå den inverkan som substratet har på hur molekylerna orienterar sig på ytan och vilka som är de viktigaste faktorerna att ta hänsyn till när man vill utforma en tillämpning.

Studera elektronerna

Den andra teknik jag har använt för att studera elektroniska egenskaper är fotoelektronspektroskopi (PES). Denna teknik baserar sig på upptäckten av den fotoelektriska effekten, som gjordes av Herz 1879, och som fick sin teoretiska tolkning av Einstein 1905. Det går att beskriva detta som att varje atom har sitt fingeravtryck. Elektronerna bildar en struktur av energinivåer och denna struktur är specifik för varje atom, t.ex. kol eller kväve eller vilken annan slags atom som helst. För att slå loss en elektron från sin elektronnivå måste

man tillföra olika mängder energi, beroende på vilken nivå det handlar om. Detta är grunden för PES. Energinivåerna i en atom ändras då den sätts in i en molekyl. Nivåerna för olika kemisk bundna atomer har olika bindningsenergi (d.v.s. den energi som åtgår för att slå loss elektronen). Genom att använda PES kan vi således se hur elektronstrukturen ändras i en molekyl när man sätter den på en yta och vi har studerat flera fall där växelverkan för Pc's med halvledarytor eller metallytor ger upphov till förändringar i elektronstrukturen som kan tolkas.

Resultat

Vi har utfört PES studier på olika typer a ftalocyaniner. Vi har studerat hur molekylerna modifieras och hur de orienterar sig beroende på val av yta. Vi har sett hur de orienterar sig annorlunda på en reaktiv yta jämfört med en icke-reaktiv sådan och hur detta leder till oordnade lager på en reaktiv yta. I STM studier har vi observerat effekten av ytan på molekylernas orientering och på hur de arrangerar sig i förhållande till varandra. I vissa fall bildar LuPc2 ordnade strukturer, men på kisel blir lagret helt oordnat. Vi har också studerat flera ftalocyaniner med metallatomer som fria molekyler i gasfas för att bättre förstå deras uppförande och den inverkan som metallatomen har.

7. Abstract in French

Cette thèse présente des résultats originaux sur les phtalocyanines (Pc) , un groupe de molécules d'inspiration biologique. En raison de l'utilisation grandissante de films moléculaires de phtalocyanine dans des dispositifs ayant des applications technologiques variées, de nombreuses études ont été consacrées à ces molécules au cours des dernières décennies.
Les spectroscopies de photoélectron sur les niveaux de cœur ou de valence (PES), la spectroscopie d'absorption des rayons X (XAS) et la microscopie à effet tunnel (STM) ont été utilisées pour étudier ces molécules en phase gazeuse et adsorbées sur l'or Au (111) et le silicium Si (100)-2$\times$1. Des calculs théoriques utilisant la fonctionnelle de la densité (DFT) sont utilisés pour obtenir des informations complémentaires sur leur structure électronique. Le but de nos études est d'obtenir une meilleure compréhension des interactions molécule - molécule et molécule - surface, pour améliorer les dispositifs à base de phtalocyanine.
Grâce à des calculs DFT et des mesures PES en phase gazeuse, il a été possible de mettre en évidence l'influence de l'ion métallique sur la bande de valence. Ainsi FePc présente les états 2p du carbone alors que ce sont les états 3d du manganèse qui dominent pour MnPc. Les études PES et STM sur H_2Pc et $LuPc_2$ déposés sur Au(111) ont révélé la formation de monocouche et de bicouche respectivement. La comparaison entre l'adsorption de $LuPc_2$ sur Si(100) nu ou passivé a confirmé la différence de réactivité sur ces deux surfaces : sur Si passivé, $LuPc_2$ conserve un caractère moléculaire, en revanche sur Si nu, une interaction importante est mise en évidence.

8. Acknowledgments

I have had the pleasure to work with the most amazing people for these four and a half years and I'm afraid that these lines won't make the justice they deserve, but I'll try my best. I would first like to thank Bernard Croset, and his fellow researchers for his warm welcome to Group of Physico-chimie des surfaces fonctionelles in INSP (UPMC), where my first steps into PhD were made. Same way I would like to thank Olof Karis and his colleagues from Molecular and Condensed matter group at Uppsala University. It was a great pleasure being part of both groups.

I'm truly grateful to my supervisors Nadine Witkowski, Carla Puglia and Nils Mårtensson. I have learned so much from You.

Nadine! I think you had the biggest part of the job to do, by showing and teaching the 'starting kit for a new scientist! The Do's and Don'ts' and I would like to think You did very well. I've learned a lot from You, starting from technical things related to UHV down to discussing weird French sayings and French cuisine.

Carla - you are amazing! You irradiate this unlimited amount of positivism from yourself, which is an amazing superpower, I have to say. And together with your passion for research - it was a true pleasure working with You and learning from You.

Nils. You 'jumped on the train' quite later, but your help has been invaluable. I truly enjoyed our conversations and was amazed every time by your ability to explain everything in such an easy way.

During these years I've crossed path with a lot of nice people, that made my days sunnier and it's impossible to name them all here on the paper, but I hope they know who they are! Nevertheless I would like to thank people without whom this thesis would not be possible (please don't mind the order):

- Yves Borensztein, Emmanuelle Lacaze, Ahmed Naitabdi, Sebastian Royer, Olivier Pluchery - whom I'm thankful for their help during different periods I spent in Paris

- Sareh Ahmadi, Mats Göthelid, Olesia Snezhkova, Nina Shariati - it was a pleasure collaborating with you.

- The staff members at Max-lab and Elettra and specially Annette Pietzsch, Joachim Schnadt, Alexei Preobrajenski, Justin Wells, Monica de Simone, Marcello Coreno, Cesare Grazioli - for helping solving the seemingly unsolvable problems (especially when it's 4am into nightshift).

- Sophie Boudet - those crazy BT and STM times I will always remember with a smile on my face.

- My 2nd family in Paris and Uppsala - Dora, Alex, Dita, Anzar, Mary J, Fafa, Josephina, Torsten, Davide, Rebecka, Kashif, Khuram - you all are amazing and you made me feel like at home.

- My fellow PhDs and friends in Paris and Uppsala - Richard, Delphine, Piotr, Amaury, Francisco, Alan, Sebastian S., Teng, Olof, Nils, Atieh, Melanie, Victor, Madeleine, Joachim, Sergey, Tobias, Anna, Ted, Jevgenija, Kaspars, Janis - you made days at work and evenings interesting and fun.

- Special thanks goes to my family for their unlimited support on my way to this point. Mam, Tēt, Sanduk, Lienit, Ūvit, paldies Jums par visu! Jūs esat mans zelts!

References

[1] A. Braun and J. Tcherniac. The products of the action of acet-anhydride on phthalamide. *Ber. Dtsch. Chem. Ges.*, 40(2), 2709–2714, 1907.

[2] G. De la Torre, C. G. Claessens, and T. Torres. Phthalocyanines: Old dyes, new materials. Putting color in nanotechnology. *Chem. Commun.*, (20), 2000, 2007.

[3] M. G. Walter, A. B. Rudine, and C. C. Wamser. Porphyrins and phthalocyanines in solar photovoltaic cells. *J. Porphyr. Phthalocya.*, 14(09), 759–792, 2010.

[4] G. Guillaud and A. Leroy. Phthalocyanine-based field-effect transistor as ozone sensor. *Sens. Actuators, B*, 73, 63–70, 2001.

[5] J. Brunet, A. Pauly, L. Mazet, J. Germain, M. Bouvet, and B. Malezieux. Improvement in real time detection and selectivity of phthalocyanine gas sensors dedicated to oxidizing pollutants evaluation. *Thin Solid Films*, 490(1), 28–35, 2005.

[6] M. Bouvet. Phthalocyanine-based field-effect transistors as gas sensors. *Anal. Bioanal. Chem.*, 384(2), 366–73, 2006.

[7] J. De Saja and M. Rodriguez-Mendez. Sensors based on double-decker rare earth phthalocyanines. *Adv. Colloid Interface Sci.*, 116(1-3), 1–11, 2005.

[8] D. Hohnholz, S. Steinbrecher, and M. Hanack. Applications of phthalocyanines in organic light emitting devices. *J. Mol. Struct.*, 521(1-3), 231–237, 2000.

[9] A. Harutyunyan, A. Kuznetsov, O. Kuznetsov, and O. Kaliya. Metal-organic magnetic materials based on cobalt phthalocyanine and possibilities of their application in medicine. *J. Magn. Magn. Mater.*, 194(1-3), 16–21, 1999.

[10] WebOfScience. http://apps.webofknowledge.com/.

[11] I. Muzikante, V. Parra, R. Dobulans, E. Fonavs, J. Latvels, and M. Bouvet. A novel gas sensor transducer based on phthalocyanine heterojunction devices. *Sensors*, 7(11), 2984–2996, November 2007.

[12] A. Generosi, B. Paci, V. R. Albertini, P. Perfetti, A. M. Paoletti, G. Pennesi, G. Rossi, and R. Caminiti. Evidence of a rearrangement of the surface structure in titanium phthalocyanine sensors induced by the interaction with nitrogen oxides molecules. *Appl. Phys. Lett.*, 87(18), 181904, 2005.

[13] M. Passard, A. Pauly, J.-P. Blanc, S. Dogo, J.-P. Germain, and C. Maleysson. Doping mechanisms of phthalocyanines by oxidizing gases: Application to gas sensors. *Thin Solid Films*, 237(1), 272–276, 1994.

[14] A. Heilmann, V. Lantto, M. Müller, and C. Hamann. NO2 monitoring as an air pollutant using lead phthalocyanine thin film sensors. *Sensor Actuat. B-Chem.*, 7, 522–525, 1992.

[15] A. M. Paoletti, G. Pennesi, G. Rossi, A. Generosi, B. Paci, and V. R. Albertini. Titanium and ruthenium phthalocyanines for NO2 Sensors: A mini-Review. *Sensors*, 9(7), 5277–5297, 2009.

[16] G. Guillaud, J. Simon, and J. Germain. Metallophthalocyanines: gas sensors, resistors and field effect transistors. *Coord. Chem. Rev.*, 178, 1433–1484, 1998.

[17] M. Bouvet, P. Gaudillat, and J.-M. Suisse. Lanthanide macrocyclic complexes: From molecules to materials and from materials to devices. *J. Porphyr. Phthalocya.*, 17, 628–635, 2013.
[18] M. Passard, J. Blanc, and C. Maleysson. Gaseous oxidation and compensating reduction of lutetium bis-phthalocyanine and lutetium phthalo-naphthalocyanine films. *Thin Solid Films*, 271(1-2), 8–14, 1995.
[19] M. Rodríguez-Méndez, J. Souto, R. de Saja, J. Martínez, and J. Antonio de Saja. Lutetium bisphthalocyanine thin films as sensors for volatile organic components (VOCs) of aromas. *Sens. Actuators, B*, 58(1-3), 544–551, 1999.
[20] N. Chaure, J. Sosa-Sanchez, A. Cammidge, M. Cook, and A. Ray. Solution processable lutetium phthalocyanine organic field-effect transistors. *Org. Electron.*, 11(3), 434–438, 2010.
[21] W. Li, A. Yu, D. C. Higgins, B. G. Llanos, and Z. Chen. Biologically inspired highly durable iron phthalocyanine catalysts for oxygen reduction reaction in polymer electrolyte membrane fuel cells. *J. Am. Chem. Soc.*, 132(48), 17056–8, 2010.
[22] P. S. Miedema, M. M. van Schooneveld, R. Bogerd, T. C. R. Rocha, M. Hävecker, A. Knop-Gericke, and F. M. F. de Groot. Oxygen binding to cobalt and iron phthalocyanines as determined from in situ X-ray absorption spectroscopy. *J. of Phys. Chem. C*, 115(51), 25422–25428, 2011.
[23] F. Sedona, M. Di Marino, D. Forrer, A. Vittadini, M. Casarin, A. Cossaro, L. Floreano, A. Verdini, and M. Sambi. Tuning the catalytic activity of Ag(110)-supported Fe phthalocyanine in the oxygen reduction reaction. *Nat. Mater.*, 11(11), 970–7, 2012.
[24] R. Cao, R. Thapa, H. Kim, X. Xu, M. Gyu Kim, Q. Li, N. Park, M. Liu, and J. Cho. Promotion of oxygen reduction by a bio-inspired tethered iron phthalocyanine carbon nanotube-based catalyst. *Nat. Commun.*, 4, 2076, 2013.
[25] C. Powell, a. Jablonski, I. Tilinin, S. Tanuma, and D. Penn. Surface sensitivity of Auger-electron spectroscopy and X-ray photoelectron spectroscopy. *J. Electron. Spectrosc. Relat. Phenom.*, 98-99, 1–15, 1999.
[26] J. Stöhr. *NEXAFS spectroscopy*. Springer Series in Surface Sciences. Springer, 2003.
[27] S. Hufner. *Photoelectron spectroscopy: Principles and applications, 2nd edition* Springer-Verlag, 1996.
[28] A. Nilson, N. Martensson. *Applications of synchrotron radiation: High-resolution studies of molecules and molecular adsorbates on surfaces*, volume Ch. 4 of *Springer Series in Surface Sciences (Book 35)*. Springer, 1994.
[29] T. D. D.P. Woodruff. *Modern techniques of surface science*. Cambridge Solid State Science Series. Cambridge University Press, 2nd edition, 1994.
[30] J. Campbell and T. Papp. Widths of the atomic K-N7 levels. *Atom. Data Nucl. Data*, 77(1), 1–56, 2001.
[31] H. Wiedemann. *Synchrotron radiation*. Springer, 2003.
[32] W. Eberhardt. *Applications of synchrotron radiation: high-resolution studies of molecules and molecular adsorbates on surfaces*. Springer Series in Surface Sciences (Book 35). Springer, 1994.
[33] G. Binnig, H. Rohrer, C. Gerber, and E. Weibel. 7x7 reconstruction on si(111) resolved in real space. *Phys. Rev. Lett.*, 50, 120–123, 1983.

[34] P. Hohenberg and W. Kohn. Inhomogenious electron gas. *Phys. Rev. B*, 136(3B), B864–&, 1964.
[35] W. Kohn and L. Sham. Self-consistent equations including exchange and correlation effects. *Phys. Rev.*, 140, 1133–1138, 1965.
[36] B. Brena. *First principles modeling of soft X-ray spectroscopy of complex systems*. PhD thesis, Royal Institute of Technology, Sweden, 2005.
[37] H. Zandvliet. Energetics of Si(001). *Rev. Mod. Phys.*, 72(2), 593–602, 2000.
[38] J. Barth, H. Brune, G. Ertl, and R. Behm. Scanning tunneling microscopy observations on the reconstructed Au(111) surface: Atomic structure, long-range superstructure, rotational domains, and surface defects. *Phys. Rev. B*, 42(15), 9307–9318, 1990.
[39] M. Debe and K. Kam. Effect of gravity on copper phthalocyanine thin films II: Spectroscopic evidence for a new oriented thin film polymorph of copper phthalocyanine grown in a microgravity enviroment. *Thin Solid Films*, 186(2), 289–325, 1990.
[40] E. A. Lucia. Spectra of polycrystalline phthalocyanines in the visible region. *J. Chem. Phys.*, 48(6), 2674, 1968.
[41] M. Passard. *Analyse et modelisation de l'action des gaz sur des semi-conducteurs organiques (phthalocyanine) pour l'application aux capteur de gaz.* PhD thesis, Universite Blaise Pascal, Clermont-Ferrand, 1995.
[42] F. Iwatsu. Size effects on the .alpha.-.beta. transformation of phthalocyanine crystals. *J. of Phys. Chem.*, 92(6), 1678–1681, 1988.
[43] P. Bassoul, M. Bouvet, and J. Simon. Relationship between the structure and the electrical properties of lutetium bisphthalocyanine thin films. *Synth. Met.*, 61(1-2), 133–137, 1993.
[44] J. Bufler, M. Abraham, M. Bouvet, J. Simon, and W. Göpel. Growth and electronic properties of ultrathin lutetium diphthalocyanine films studied by electron spectroscopy. *J. Chem. Phys.*, 95(11), 8459–8466, 1991.
[45] P. Palmgren, B. Priya, N. Niraj, and M. Göthelid. Self-ordering of metal-free phthalocyanine on InAs (100) and InSb (100). *J. Phys.: Condens. Matter*, 18, 10707, 2006.
[46] X. Lu and K. W. Hipps. Scanning tunneling microscopy of metal phthalocyanines: d 6 and d 8 Cases. *J. Phys. Chem. B*, 101(27), 5391–5396, 1997.
[47] G. Dufour, C. Poncey, F. Rochet, H. Roulet, M. Sacchi, M. De Santis, and M. De Crescenzi. Copper phthalocyanine on Si(111)-7x7 and Si(001)-2x1 surfaces: an X-ray photoemission spectroscopy and synchrotron X-ray absorption spectroscopy study. *Surf. Sci.*, 319(3), 251–266, 1994.
[48] M. Takada and H. Tada. Low temperature scanning tunneling microscopy of phthalocyanine multilayers on au(111) surfaces. *Chem. Phys. Lett.*, 392, 265–269, 2004.
[49] Y. Kanemitsu, A. Yamamoto, H. Funada, and Y. Masumoto. Photocarrier generation in metal-free phthalocyanines: Effect of the stacking habit of molecules on the photogeneration efficiency. *J. Appl. Phys.*, 69(10), 7333, 1991.
[50] O. Berger, W.-J. Fischer, B. Adolphi, S. Tierbach, V. Melev, and J. Schreiber. Studies on phase transformations of Cu-phthalocyanine thin films. *J. Mater. Sci.: Mater. Electron.*, 11(4), 331–346, 2000.

[51] M. Brinkmann, J. Wittmann, C. Chaumont, and J. André. Effects of solvent on the morphology and crystalline structure of lithium phthalocyanine thin films and powders. *Thin Solid Films*, 292(1), 192–203, 1997.

[52] Z. Lu, C. Zhan, X. Yu, W. He, H. Jia, L. Chen, A. Tang, J. Huang, and J. Yao. Large-scale, ultra-dense and vertically standing zinc phthalocyanine π-π stacks as a hole-transporting layer on an ITO electrode. *J. Mater. Chem.*, 22(44), 23492, 2012.

[53] T. Wang, Y. Zhu, and Q. Jiang. Molecular orientation transformation in initial growth stage of disk-like phthalocyanine during organic vapor deposition process. *Chem. Sci.*, 3, 528, 2012.

[54] R. Blyth, R. Delaunay, M. Zitnik, J. Krempasky, R. Krempaska, J. Slezak, K. Prince, R. Richter, M. Vondracek, R. Camilloni, L. Avaldi, M. Coreno, G. Stefani, C. Furlani, M. de Simone, S. Stranges, and M.-Y. Adam. The high resolution gas phase photoemission beamline, Elettra. *J. Electron Spectrosc. Relat. Phenom.*, 101, 959–964, 1999.

[55] R. Denecke, P. Väterlein, M. Bässler, N. Wassdahl, S. Butorin, A. Nilsson, J. E. Rubensson, J. Nordgren, N. Mårtensson, and R. Nyholm. Beamline I511 at MAX II, capabilities and performance. *J. Electron Spectrosc. Relat. Phenom.*, 101, 971–977, 1999.

[56] J. Schnadt, J. Knudsen, J. N. Andersen, H. Siegbahn, A. Pietzsch, F. Hennies, N. Johansson, N. Mårtensson, G. Ohrwall, S. Bahr, S. Mähl, and O. Schaff. The new ambient-pressure X-ray photoelectron spectroscopy instrument at MAX-lab. *J Synchrotron Radiat.*, 19, 701–4, 2012.

[57] C. Mathieu, X. Bai, J.-J. J. Gallet, F. Bournel, S. Carniato, F. Rochet, E. Magnano, F. Bondino, R. Funke, U. Kohler, and S. Kubsky. Molecular staples on Si(001)-2x1: Dual-head primary amines. *J. Phys. Chem. C*, 113(26), 11336–11345, 2009.

[58] S. Tanuma, C. J. Powell, and D. R. Penn. Proposed formula for electron inelastic mean free paths based on calculations for 31 materials. *Surf. Sci.*, 192(1), 849–857, 1987.

[59] S. Kera, M. Casu, K. Bauchspieß, D. Batchelor, T. Schmidt, and E. Umbach. Growth mode and molecular orientation of phthalocyanine molecules on metal single crystal substrates: A NEXAFS and XPS study. *Surf. Sci.*, 600(5), 1077–1084, 2006.

Acta Universitatis Upsaliensis

Digital Comprehensive Summaries of Uppsala Dissertations from the Faculty of Science and Technology 1119

Editor: The Dean of the Faculty of Science and Technology

A doctoral dissertation from the Faculty of Science and Technology, Uppsala University, is usually a summary of a number of papers. A few copies of the complete dissertation are kept at major Swedish research libraries, while the summary alone is distributed internationally through the series Digital Comprehensive Summaries of Uppsala Dissertations from the Faculty of Science and Technology.

Distribution: publications.uu.se
urn:nbn:se:uu:diva-217086

ACTA
UNIVERSITATIS
UPSALIENSIS
UPPSALA
2014